

ROBUST STABILITY AND PRECONDITIONING OF DARCY–FORCHHEIMER EQUATIONS*

RISHI DAS[†], HARSHA HUTRIDURGA[‡], AMIYA K. PANI[§], AND RICARDO RUIZ-BAIER[¶]

Abstract. We derive parameter-robust quasi-optimal error estimates for mixed finite element methods for the nonlinear Darcy–Forchheimer equations with mixed boundary conditions. Using the framework of operator preconditioning, we also design efficient block preconditioners for the linearised system, that exhibit robustness with respect to the coefficients that modulate permeability and inertia of the system. The properties of the formulation (parameter and mesh-size independence of the convergence rates) are illustrated by means of several numerical examples.

Key words. A priori error analysis, mixed finite element methods, nonlinear flow in porous media, robust preconditioning.

AMS subject classifications. 65N30, 65N12, 65N15.

1. Introduction.

Scope. The Darcy–Forchheimer equations model fluid flow through porous media, when both viscous and inertial effects are significant. While Darcy’s law describes the linear flow proportional to the pressure gradient and is valid for slow, creeping flows, the Forchheimer extension introduces a nonlinear correction to account for inertial effects (manifesting itself as term depending as a power law on the velocity magnitude, taking into account kinematic energy loss) that arise at moderate flow velocities. These equations have broad applications in engineering and geosciences (high-velocity subsurface flows such as near injection or extraction wells in gas reservoirs and conglomerate-confined aquifers, contaminant transport in environmental engineering, and in filtration and catalytic bed reactors in chemical engineering) [26, 29], as well as in biological systems (e.g., blood perfusion in tissues, where nonlinearity in flow resistance can be significant) [19, 21].

Mixed finite element methods provide a natural framework for the numerical approximation of Darcy–Forchheimer flows, as they offer local mass conservation and accurate flux approximations. Their construction and analysis have been addressed through fixed-point and Newton methods [1, 3, 27, 31, 18, 24, 12], often coupled with iterative solvers tailored to the nonlinear structure.

For Darcy and Forchheimer-type equations, which model creeping and inertial flows, respectively, the associated saddle-point systems exhibit strong sensitivity to variations in physical parameters such as permeability and the Forchheimer coefficient. Robust iterative solvers require preconditioners that maintain spectral equivalence independently of these parameters. For this, we follow the framework of operator preconditioning from [28] (see, also the earlier works [25, 2]), which suggests linking the

*Updated: October 28, 2025.

Funding: This work has been partially supported by the Australian Research Council through the FUTURE FELLOWSHIP grant FT220100496 and DISCOVERY PROJECT grant DP22010316.

[†] IITB–Monash Research Academy, Indian Institute of Technology Bombay, Powai, Mumbai, Maharashtra 400076, India (rishi.das@iitb.ac.in).

[‡]Department of Mathematics, Indian Institute of Technology Bombay, Powai, Mumbai, Maharashtra 400076, India (harsha@math.iitb.ac.in).

[§]Department of Mathematics, BITS-Pilani, KK Birla Goa Campus, Zuarinagar, Goa-403726, India (amiyap@goa.bits-pilani.ac.in).

[¶]Corresponding author: School of Mathematics, Monash University, 9 Rainforest Walk, Melbourne VIC 3800, Australia (ricardo.ruizbaier@monash.edu).

preconditioning of algebraic systems with their infinite-dimensional operator counterpart. This allows to construct preconditioners by approximating the Riesz maps of the continuous operators in appropriate function space norms (or duality maps in the case of Banach spaces). For the mixed formulation of the Darcy problem, this approach yields block-diagonal preconditioners involving sums of spaces of pressure, as developed in [5] (and also extended for Biot equations and other families of perturbed saddle-point problems in, e.g., [8, 10, 23]). However, these works do not address in details the error analysis, which is also expected to maintain parameter robustness.

The objective of this work is twofold. First, to specify Céa-type estimates and convergence rates using the parameter-weighted norms, and secondly, to apply this approach to a (relatively simple) nonlinear extension to Darcy–Forchheimer flow equations. Obtaining uniform stability with respect to model parameters is of great interest for multiphysics coupling models since the variation of coefficients across sub-domains, or spatial scales, or different applications, can be extremely large. Also, coupling through interfaces with other flow regimes typically implies that we cannot simply rescale one equation, but certain compatibility of the parametrisation of both sub-models must be maintained.

While operator preconditioning techniques are available for many linear elliptic and saddle point problems, developing such robust solvers for general nonlinear saddle point problems exhibits significant challenges. Available techniques include multilevel, domain decomposition, operator preconditioning in the Hilbert context, field-split algorithms, and Sobolev gradient methods, for example (see, the review in [14]). In the nonlinear Forchheimer regime, linearisation techniques (e.g., Picard or Newton) give rise to a sequence of linearised problems, for which an operator preconditioning approach can be extended using variable-coefficient norm scalings following [33]. Inspired by [32] for multiphysics couplings, using the norms induced by the parameter-robust stability analysis, this paper proposes and analyse simple block diagonal (variable) operator preconditioners for the linearised Darcy–Forchheimer system.

In order to deal with intersections and sums of parameter-weighted function spaces, from [28, 8], it is possible to prove continuous and discrete inf-sup conditions by carefully combining auxiliary PDEs with different regularity and parameter weighting. This approach also requires a lifting map, and then, appropriate maps are constructed using the aforementioned auxiliary problems. Based on similar techniques, here we first discuss well-posedness of three different suitable PDEs and secondly, derive the inf-sup stability using a lifting map in the discrete case.

Outline. The remainder of the paper is organised in the following manner. Section 2 recalls the necessary notations, the boundary value problem and the derivation of the weak formulation using parameter-weighted norms. Section 3 addresses the well-posedness of the weak formulation robustly with respect to model parameters, following the abstract theory of Minty–Browder monotone operators. In Section 4, we discuss the robust solvability of the discrete problem. In addition, we present quasi-optimal error analysis and derive precise convergence rates for conforming discretisations of the nonlinear model in Section 4.2. Next, in Section 5 we discuss how a simple variable operator preconditioning can be used in this context of Banach spaces, and we conclude in Section 6 with a set of numerical tests illustrating the properties of the proposed schemes.

2. Model problem.

Notation and preliminaries. Let $\Omega \subset \mathbb{R}^d$, $d \in \{2, 3\}$, denote a bounded domain with Lipschitz-continuous boundary $\partial\Omega$, on which its outward unit normal is denoted

by \mathbf{n} . For $s \geq 0$ and $r \in [1, +\infty]$, we denote by $L^r(\Omega)$ and $W^{s,r}(\Omega)$ the usual Lebesgue and Sobolev spaces endowed with the norms $\|\bullet\|_{0,r,\Omega}$ and $\|\bullet\|_{s,r,\Omega}$, respectively. Note that $W^{0,r}(\Omega) = L^r(\Omega)$. If $r = 2$, we write $H^s(\Omega)$ in place of $W^{s,2}(\Omega)$, and denote the corresponding norm by $\|\bullet\|_{s,\Omega}$. We denote by \mathbf{H} the vectorial counterpart of a generic scalar functional space H . The $L^2(\Omega)$ inner product for scalar, vector, or tensor valued functions is denoted by $(\bullet, \bullet)_{0,\Omega}$. We also recall the Hilbert space $\mathbf{H}(\text{div}, \Omega) = \{\mathbf{v} \in \mathbf{L}^2(\Omega) : \text{div } \mathbf{v} \in L^2(\Omega)\}$ endowed with the norm $\|\mathbf{v}\|_{\text{div},\Omega}^2 = \|\mathbf{v}\|_{0,\Omega}^2 + \|\text{div } \mathbf{v}\|_{0,\Omega}^2$. Moreover, we use for $r, s \in [1, +\infty)$, the Banach space

$$\mathbf{H}^r(\text{div}_s, \Omega) = \{\mathbf{v} \in \mathbf{L}^r(\Omega) : \text{div } \mathbf{v} \in \mathbf{L}^s(\Omega)\},$$

endowed with the norm $\|\mathbf{v}\|_{r,\text{div}_s,\Omega}^2 = \|\mathbf{v}\|_{0,r,\Omega}^r + \|\text{div } \mathbf{v}\|_{0,s,\Omega}^s$. Often, we use a subscript Γ_i on the functional space to denote that the (appropriate) traces vanish on the part of the boundary $\Gamma_i \subset \partial\Omega$.

For two Banach spaces $(X, \|\bullet\|_X)$ and $(Y, \|\bullet\|_Y)$, we denote by $\mathcal{L}(X, Y)$ the space of bounded linear maps from X to Y . Let $(Z, \|\bullet\|_Z)$ be another Banach space. The intersection and sum spaces are

$$X \cap Y \cap Z = \{v : v \in X \text{ and } v \in Y \text{ and } v \in Z\},$$

$$X + Y + Z = \{u + v + w : u \in X \text{ and } v \in Y \text{ and } w \in Z\},$$

and their respective norms are (see [5], noting that the same norm characterisation done there for Hilbert spaces holds also for the Banach case)

$$\|r\|_{X \cap Y \cap Z}^2 = \|r\|_X^2 + \|r\|_Y^2 + \|r\|_Z^2, \quad \|z\|_{X+Y+Z}^2 = \inf_{\substack{r=u+v+w, \\ u \in X, v \in Y, w \in Z}} [\|u\|_X^2 + \|v\|_Y^2 + \|w\|_Z^2].$$

Furthermore, if $X \cap Y \cap Z$ is dense in X and Y and Z , then following relation (understood as an identification under an isometry) holds

$$(X + Y + Z)' = X' \cap Y' \cap Z'. \tag{2.1}$$

In addition, for a fixed positive constant α , by αX we denote the Banach space whose elements coincide with those in X but are measured with the norm

$$\|\bullet\|_{\alpha X}^2 = \alpha^2 \|\bullet\|_X^2.$$

Strong form of the governing equations. We assume that the domain boundary $\partial\Omega$ is decomposed between two sub-boundaries Γ_u and Γ_p , both with positive $(d-1)$ -Hausdorff measure. The governing equations consist in finding the discharge flux \mathbf{u} and pressure head p satisfying

$$\kappa^{-1} \mathbf{u} + F |\mathbf{u}|^{r-2} \mathbf{u} + \nabla p = \mathbf{f} \quad \text{in } \Omega, \tag{2.2a}$$

$$\text{div } \mathbf{u} = g \quad \text{in } \Omega, \tag{2.2b}$$

$$\mathbf{u} \cdot \mathbf{n} = 0 \quad \text{on } \Gamma_u, \tag{2.2c}$$

$$p = 0 \quad \text{on } \Gamma_p. \tag{2.2d}$$

Here, κ is the hydraulic conductivity (permeability of the porous matrix divided by the fluid viscosity), \mathbf{f} is a forcing vector, g is a fluid source, and $F > 0$, $r \in [3, 4]$ are the Forchheimer coefficient and index, respectively.

Regarding the weak formulation of (2.2), we now consider generic spaces \mathbf{V} and Q for velocity and pressure, respectively (and to be made precise below), yielding: Find $(\mathbf{u}, p) \in \mathbf{V} \times Q$ such that

$$a(\mathbf{u}, \mathbf{v}) + c(\mathbf{u}; \mathbf{u}, \mathbf{v}) + b(\mathbf{v}, p) = F(\mathbf{v}) \quad \forall \mathbf{v} \in \mathbf{V}, \quad (2.3a)$$

$$b(\mathbf{u}, q) = G(q) \quad \forall q \in Q, \quad (2.3b)$$

where for sufficiently regular \mathbf{V} (incorporating the flux boundary condition in an essential manner) and Q , the following bilinear forms $a : \mathbf{V} \times \mathbf{V} \rightarrow \mathbb{R}$, $b : \mathbf{V} \times Q \rightarrow \mathbb{R}$, linear functionals $F : \mathbf{V} \rightarrow \mathbb{R}$, $G : Q \rightarrow \mathbb{R}$, and nonlinear form $c : \mathbf{V} \times \mathbf{V} \times \mathbf{V} \rightarrow \mathbb{R}$, are defined, respectively, as:

$$\begin{aligned} a(\mathbf{u}, \mathbf{v}) &:= \int_{\Omega} \kappa^{-1} \mathbf{u} \cdot \mathbf{v}, \quad b(\mathbf{v}, q) := \int_{\Omega} q \operatorname{div} \mathbf{v}, \quad F(\mathbf{v}) := \int_{\Omega} \mathbf{f} \cdot \mathbf{v}, \\ G(q) &:= \int_{\Omega} g q, \quad c(\mathbf{w}; \mathbf{u}, \mathbf{v}) := \int_{\Omega} \mathbf{F} |\mathbf{w}|^{r-2} \mathbf{u} \cdot \mathbf{v}. \end{aligned}$$

3. Continuous robust solvability. First, we recall an abstract setting and its solvability using the Minty–Browder framework, which we shall use it for the well-posedness of (2.3). A proof can be found in, e.g., [11, Theorem 3.1] (see also [12, Theorem 3.1]).

THEOREM 3.1 (Abstract setting for well-posedness). *Let X, Y be two reflexive Banach spaces, $\mathcal{A} : X \rightarrow X'$ a nonlinear map, $\mathcal{B} : X \rightarrow Y'$ a linear and bounded operator, and denote by $Z := \{v \in X : \mathcal{B}(v) = 0\}$ the kernel of \mathcal{B} . Assume that*

- (*Local Lipschitz continuity*). *There exist $\gamma > 0$ and $s \geq 2$ such that*

$$\|\mathcal{A}(u) - \mathcal{A}(v)\|_{X'} \leq \gamma \|u - v\|_X + \gamma \|u - v\|_X (\|u\|_X + \|v\|_X)^{s-2} \quad \forall u, v \in X.$$

- (*Uniformly strong monotonicity on the kernel*). *For a fixed $w \in X$, there exists $\alpha > 0$ such that*

$$\langle \mathcal{A}(u + w) - \mathcal{A}(v + w), u - v \rangle \geq \alpha \|u - v\|_X^2 \quad \forall u, v \in Z.$$

- (*Inf-sup stability*). *There exists $\beta > 0$ such that*

$$\sup_{\substack{v \in X \\ v \neq 0}} \frac{\langle \mathcal{B}(v), q \rangle}{\|v\|_X} \geq \beta \|q\|_Y \quad \forall q \in Y.$$

Then, for each $(f, g) \in X' \times Y'$ there exists a unique $(u, p) \in X \times Y$ such that

$$\begin{aligned} \langle \mathcal{A}(u), v \rangle + \langle \mathcal{B}(v), p \rangle &= \langle f, v \rangle \quad \forall v \in X, \\ \langle \mathcal{B}(u), q \rangle &= \langle g, q \rangle \quad \forall q \in Y. \end{aligned}$$

Moreover, there exists $C > 0$, depending only on α, γ, β , and s such that

$$\|(u, p)\|_{X \times Y} \leq C(\mathcal{M}(f, g) + \{\mathcal{M}(f, g)\}^{s-1}), \quad (3.1)$$

where $\mathcal{M}(f, g) := \|f\|_{X'} + \|g\|_{Y'} + \|g\|_{Y'}^{s-1} + \|\mathcal{A}(0)\|_{X'}$.

We now remark that Theorem 3.1 readily yields the unique solvability of (2.3) if we specify the spaces $\mathbf{V} = \mathbf{H}_{\Gamma_u}^3(\operatorname{div}, \Omega)$ and $Q = L^2(\Omega)$ and this has been established in, e.g., [31]. However, the properties of the weak formulation (in particular, uniformly

strong monotonicity on the kernel and inf-sup condition) are not necessarily uniform with respect to the model parameters, leading to lack of parameter robustness of the corresponding continuous dependence on data.

We adapt the operator preconditioning approach from [28] (and used for Darcy equations in [5]) and proceed first to show an auxiliary property of the divergence operator that will allow us to show a parameter-robust inf-sup condition.

LEMMA 3.2. *There exists an operator \mathcal{S}_c satisfying the following properties:*

$$\begin{aligned} \mathcal{S}_c \in \mathcal{L}(Q', \mathbf{V}), \quad & \|\mathcal{S}_c\|_{\mathcal{L}(Q', \mathbf{V})} \text{ is independent of } \kappa, F, \quad \text{and} \\ (\operatorname{div}[\mathcal{S}_c(g)], \psi) = \langle g, \psi \rangle \quad & \text{for all } g \in Q', \psi \in Q. \end{aligned} \quad (3.2)$$

Proof. We proceed to define \mathcal{S}_c as a bounded linear operator from three different spaces, and then, invoke the duality relation between sum and intersection between Banach spaces (2.1) to conclude that $\mathcal{S}_c \in \mathcal{L}(Q', \mathbf{V})$.

For the existence of $\mathcal{S}_c \in \mathcal{L}((W_{\Gamma_p}^{1,q}(\Omega))', \mathbf{L}^r(\Omega))$ with $q \in \{2, \frac{3}{2}\}$, let $\phi \in W_{\Gamma_p}^{1,r}(\Omega)$ for a given $g \in (W_{\Gamma_p}^{1,q}(\Omega))'$ with $\frac{1}{q} + \frac{1}{r} = 1$ be a unique weak solution of the following elliptic problem with mixed boundary conditions (owing to, e.g., [30, Chapter 7])

$$-\Delta\phi = g \quad \text{in } \Omega, \quad \nabla\phi \cdot \mathbf{n} = 0 \quad \text{on } \Gamma_u, \quad \phi = 0 \quad \text{on } \Gamma_p. \quad (3.3)$$

Then, it suffices to define $\mathcal{S}_c(g) := \nabla\phi$, where $\nabla\phi \in \mathbf{L}^r(\Omega)$. This, in turn, shows $\mathcal{S}_c \in \mathcal{L}((W_{\Gamma_p}^{1,q}(\Omega))', \mathbf{L}^r(\Omega))$, for $q = 2$ and $q = \frac{3}{2}$ corresponding to $r = 2$ and 3 , respectively.

Now, for $g \in (L^2(\Omega))'$, let $(\mathbf{w}, r) \in \mathbf{H}_{\Gamma_u}(\operatorname{div}, \Omega) \times L^2(\Omega)$ be the unique solution (cf. [7, Section 7.1.2]) of

$$(\mathbf{w}, \mathbf{z}) + (\operatorname{div} \mathbf{z}, r) = 0 \quad \forall \mathbf{z} \in \mathbf{H}_{\Gamma_u}(\operatorname{div}, \Omega), \quad (3.4a)$$

$$(\operatorname{div} \mathbf{w}, s) = \langle g, s \rangle \quad \forall s \in L^2(\Omega). \quad (3.4b)$$

Then, we note that \mathcal{S}_c can also be defined as $\mathcal{S}_c(g) := \mathbf{w}$, and therefore,

$$\mathcal{S}_c \in \mathcal{L}(L^2(\Omega), \mathbf{H}_{\Gamma_u}(\operatorname{div}, \Omega)). \quad (3.5)$$

This completes the proof. \square

For a robust well-posedness of the Darcy–Forchheimer formulation, consider the following weighted spaces

$$\mathbf{V} = \kappa^{-\frac{1}{2}} \mathbf{L}^2(\Omega) \cap \mathbf{H}_{\Gamma_u}(\operatorname{div}, \Omega) \cap F^{\frac{1}{3}} \mathbf{L}^3(\Omega), \quad Q = L^2(\Omega) + \kappa^{\frac{1}{2}} H_{\Gamma_p}^1(\Omega) + F^{-\frac{1}{3}} W_{\Gamma_p}^{1, \frac{3}{2}}(\Omega),$$

endowed with the following norms

$$\|\mathbf{v}\|_{\mathbf{V}} := \kappa^{-\frac{1}{2}} \|\mathbf{v}\|_{0,\Omega} + \|\operatorname{div} \mathbf{v}\|_{0,\Omega} + F^{\frac{1}{3}} \|\mathbf{v}\|_{0,3,\Omega}, \quad (3.6a)$$

$$\|q\|_Q := \inf_{\substack{q=q_1+q_2+q_3, \\ (q_1, q_2, q_3) \in L^2(\Omega) \times H_{\Gamma_p}^1(\Omega) \times W_{\Gamma_p}^{1, \frac{3}{2}}(\Omega)}} [\|q_1\|_{0,\Omega} + \kappa^{\frac{1}{2}} \|q_2\|_{1,\Omega} + F^{-\frac{1}{3}} \|q_3\|_{1, \frac{3}{2}, \Omega}], \quad (3.6b)$$

respectively.

THEOREM 3.3 (Parameter-robust well-posedness). *Assume that $\mathbf{f} \in \mathbf{L}^2(\Omega)$, $g \in L^2(\Omega)$. Then, there exists a unique pair of solutions $(\mathbf{u}, p) \in \mathbf{V} \times Q$ to the problem (2.3). Furthermore, there is a positive constant \tilde{C} , independent of the model parameters κ, F , such that*

$$\|(\mathbf{u}, p)\|_{\mathbf{V} \times Q} \leq \tilde{C} \max\{(\|\mathbf{f}\|_{0,\Omega} + \|g\|_{0,\Omega} + \|g\|_{0,\Omega}^2), (\|\mathbf{f}\|_{0,\Omega} + \|g\|_{0,\Omega} + \|g\|_{0,\Omega}^2)\}.$$

Proof. In order to apply Theorem 3.1, we define the operators $A : \mathbf{V} \rightarrow \mathbf{V}'$, $B : \mathbf{V} \rightarrow \mathbf{Q}'$, and $C : \mathbf{V} \rightarrow \mathbf{V}'$ as $\langle A\mathbf{u}, \mathbf{w} \rangle := a(\mathbf{u}, \mathbf{w})$, $\langle B\mathbf{v}, p \rangle := b(\mathbf{v}, p)$, and $\langle C(\mathbf{u}), \mathbf{w} \rangle := c(\mathbf{u}; \mathbf{u}, \mathbf{w})$, respectively. Now, set the non-linear operator $A + C : \mathbf{V} \rightarrow \mathbf{V}'$. We proceed to verify the assumptions of Theorem 3.1 identifying $X \equiv \mathbf{V}$, $Y \equiv \mathbf{Q}$, $\mathcal{A} \equiv A + C$, $\mathcal{B} \equiv B$, and $s = 3$.

Local Lipschitz continuity. For $\mathbf{u}, \mathbf{v}, \mathbf{w} \in \mathbf{V}$, apply Hölder's inequality to obtain

$$\begin{aligned} \langle \{A + C\}(\mathbf{u}), \mathbf{w} \rangle - \langle \{A + C\}(\mathbf{v}), \mathbf{w} \rangle &= \int_{\Omega} \kappa^{-1}(\mathbf{u} - \mathbf{v}) \cdot \mathbf{w} + \int_{\Omega} F(|\mathbf{u}| \mathbf{u} - |\mathbf{v}| \mathbf{v}) \cdot \mathbf{w} \\ &\leq \kappa^{-\frac{1}{2}} \|\mathbf{u} - \mathbf{v}\|_{0,\Omega} \kappa^{-\frac{1}{2}} \|\mathbf{w}\|_{0,\Omega} + F^{\frac{1}{3}} \|\mathbf{w}\|_{0,3,\Omega} F^{\frac{2}{3}} \|\mathbf{u}| \mathbf{u} - |\mathbf{v}| \mathbf{v}\|_{0,\frac{3}{2},\Omega}. \end{aligned}$$

Using [6, Lemma 2.1, equation (2.1a)] to bound the second term on the right-hand side of the above expression, we deduce that there exists a positive constant \tilde{C} independent of κ, F , such that

$$\begin{aligned} &\langle \{A + C\}(\mathbf{u}), \mathbf{w} \rangle - \langle \{A + C\}(\mathbf{v}), \mathbf{w} \rangle \\ &\leq \kappa^{-\frac{1}{2}} \|\mathbf{u} - \mathbf{v}\|_{0,\Omega} \kappa^{-\frac{1}{2}} \|\mathbf{w}\|_{0,\Omega} + F^{\frac{1}{3}} \|\mathbf{w}\|_{0,3,\Omega} \tilde{C} F^{\frac{1}{3}} (\|\mathbf{u}\|_{0,3,\Omega} + \|\mathbf{v}\|_{0,3,\Omega}) F^{\frac{1}{3}} \|\mathbf{u} - \mathbf{v}\|_{0,3,\Omega} \\ &\leq \|\mathbf{u} - \mathbf{v}\|_{\mathbf{V}} \|\mathbf{w}\|_{\mathbf{V}} + \tilde{C} (\|\mathbf{u}\|_{\mathbf{V}} + \|\mathbf{v}\|_{\mathbf{V}}) \|\mathbf{u} - \mathbf{v}\|_{\mathbf{V}} \|\mathbf{w}\|_{\mathbf{V}}, \end{aligned}$$

and therefore, there holds

$$\|\{A + C\}(\mathbf{u}) - \{A + C\}(\mathbf{v})\|_{\mathbf{V}'} \leq \|\mathbf{u} - \mathbf{v}\|_{\mathbf{V}} + \tilde{C} (\|\mathbf{u}\|_{\mathbf{V}} + \|\mathbf{v}\|_{\mathbf{V}}) \|\mathbf{u} - \mathbf{v}\|_{\mathbf{V}}. \quad (3.7)$$

Uniformly strong monotonicity of $\{A + C\}(\bullet + \mathbf{w})$. First we stress that for all $\mathbf{u} \in \mathbf{Z} := \{\mathbf{v} \in \mathbf{V} : b(\mathbf{v}, q) = 0 \quad \forall q \in \mathbf{Q}\}$, we can choose $q = \operatorname{div} \mathbf{u} \in L^2(\Omega) \subseteq \mathbf{Q}$ and therefore, we have the characterisation $\mathbf{Z} = \{\mathbf{v} \in \mathbf{V} : \operatorname{div} \mathbf{v} = 0\}$. Now, for $\mathbf{u}, \mathbf{v} \in \mathbf{Z}$ and $\mathbf{w} \in \mathbf{V}$, it holds

$$\begin{aligned} &\langle \{A + C\}(\mathbf{u} + \mathbf{w}) - \{A + C\}(\mathbf{v} + \mathbf{w}), \mathbf{u} - \mathbf{v} \rangle \\ &= \int_{\Omega} \kappa^{-1} |\mathbf{u} - \mathbf{v}|^2 + F \int_{\Omega} ((\mathbf{u} + \mathbf{w})|\mathbf{u} + \mathbf{w}| - (\mathbf{v} + \mathbf{w})|\mathbf{v} + \mathbf{w}|) \cdot (\mathbf{u} - \mathbf{v}). \end{aligned}$$

By employing [6, Lemma 2.1 and (2.1b)], we deduce that there exists a constant $\tilde{C} > 0$ depending only on the volume of Ω , such that

$$F \int_{\Omega} ((\mathbf{u} + \mathbf{w})|\mathbf{u} + \mathbf{w}| - (\mathbf{v} + \mathbf{w})|\mathbf{v} + \mathbf{w}|) \cdot (\mathbf{u} - \mathbf{v}) \geq \tilde{C} F \|\mathbf{u} - \mathbf{v}\|_{0,3,\Omega}^3$$

Finally, from the above inequality, taking $\alpha^{\frac{1}{2}} = \min\{1, \tilde{C}^{\frac{1}{3}}\}$, it follows that

$$\langle \{A + C\}(\mathbf{u} + \mathbf{w}) - \{A + C\}(\mathbf{v} + \mathbf{w}), \mathbf{u} - \mathbf{v} \rangle \geq \alpha \|\mathbf{u} - \mathbf{v}\|_{\mathbf{V}}^2, \quad (3.8)$$

where, we have used that the $\mathbf{H}(\operatorname{div})$ -seminorm is zero since $\mathbf{u}, \mathbf{v} \in \mathbf{Z}$.

Inf-sup stability. From the existence of the map \mathcal{S}_c defined in Lemma 3.2, it immediately follows that

$$\begin{aligned} \sup_{\mathbf{0} \neq \mathbf{v} \in \mathbf{V}} \frac{(\operatorname{div} \mathbf{v}, p)}{\|\mathbf{v}\|_{\mathbf{V}}} &\geq \sup_{g \in \mathbf{Q}'} \frac{(\operatorname{div} \mathcal{S}_c(g), p)}{\|\mathcal{S}_c(g)\|_{\mathbf{V}}} = \sup_{g \in \mathbf{Q}'} \frac{\langle g, p \rangle}{\|\mathcal{S}_c(g)\|_{\mathbf{V}}} \\ &\geq \|\mathcal{S}_c\|_{\mathcal{L}(\mathbf{Q}', \mathbf{V})}^{-1} \sup_{g \in \mathbf{Q}'} \frac{\langle g, p \rangle}{\|g\|_{\mathbf{Q}'}} = \beta \|p\|_{\mathbf{Q}}, \end{aligned}$$

where $\beta = \|\mathcal{S}_c\|_{\mathcal{L}(Q', \mathbf{V})}^{-1}$ is independent of the parameters κ, F , and hence, the inf-sup condition is satisfied.

An appeal to the Theorem 3.1 implies the existence of a unique velocity-pressure pair of solutions to the problem (2.3).

In order to complete the proof, it remains to show the continuous dependence of $\|(\mathbf{u}, p)\|_{\mathbf{V} \times Q}$ on the data. From (2.3a), we arrive at $B^*(p) = F - \{A + C\}(\mathbf{u})$, and the inf-sup stability of B shows

$$\|p\|_Q \leq \frac{1}{\beta} \|B^*(p)\|_{\mathbf{V}} \leq \{\|F\|_{\mathbf{V}'} + \|\{A + C\}(\mathbf{u})\|_{\mathbf{V}'}\}. \quad (3.9)$$

Also, the surjectivity of B implies that since $G \in Q'$ in (2.3b), there exists a unique $\hat{\mathbf{u}} \in \mathbf{V} \setminus \mathbf{Z}$, such that $\mathbf{u} = \tilde{\mathbf{u}} + \hat{\mathbf{u}}$, where $\tilde{\mathbf{u}} \in \mathbf{Z}$,

$$B(\hat{\mathbf{u}}) = G \quad \text{and} \quad \|\hat{\mathbf{u}}\|_{\mathbf{V}} \leq \frac{1}{\beta} \|G\|_{Q'}.$$

Now, for the uniformly strong monotonicity of $A + C$ (cf. (3.8)), we choose $\mathbf{u} = \tilde{\mathbf{u}}, \mathbf{v} = \mathbf{0}$ and $\mathbf{w} = -\hat{\mathbf{u}}$, and then for equation (2.3a), we set $\mathbf{v} = \tilde{\mathbf{u}}$. Further, we use the local Lipschitz continuity of A , by setting $\mathbf{v} = \mathbf{0}$ in (3.7), to conclude that

$$\begin{aligned} \alpha \|\tilde{\mathbf{u}}\|_{\mathbf{V}}^2 &\leq \langle \{A + C\}(\tilde{\mathbf{u}} + \hat{\mathbf{u}}) - \{A + C\}(\mathbf{0} + \hat{\mathbf{u}}), \tilde{\mathbf{u}} \rangle \\ &\leq \{\|F\|_{\mathbf{V}'} + \|\{A + C\}(\hat{\mathbf{u}})\|_{\mathbf{V}'}\} \|\tilde{\mathbf{u}}\|_{\mathbf{V}} \\ &\leq \{\|F\|_{\mathbf{V}'} + \|\hat{\mathbf{u}}\|_{\mathbf{V}} + \|\hat{\mathbf{u}}\|_{\mathbf{V}}^2\} \|\tilde{\mathbf{u}}\|_{\mathbf{V}} \leq \{\|F\|_{\mathbf{V}'} + \frac{1}{\beta} \|G\|_{Q'} + \frac{1}{\beta^2} \|G\|_{Q'}^2\} \|\tilde{\mathbf{u}}\|_{\mathbf{V}}, \end{aligned}$$

and hence,

$$\|\tilde{\mathbf{u}}\|_{\mathbf{V}} \leq \frac{1}{\alpha} \{\|F\|_{\mathbf{V}'} + \frac{1}{\beta} \|G\|_{Q'} + \frac{1}{\beta^2} \|G\|_{Q'}^2\}. \quad (3.10)$$

Finally, from (3.10), using the triangle inequality, we find that

$$\|\mathbf{u}\|_{\mathbf{V}} \leq \|\tilde{\mathbf{u}}\|_{\mathbf{V}} + \|\hat{\mathbf{u}}\|_{\mathbf{V}} \leq \frac{1}{\alpha} \{\|F\|_{\mathbf{V}'} + \frac{1+\alpha}{\beta} \|G\|_{Q'} + \frac{1}{\beta^2} \|G\|_{Q'}^2\}. \quad (3.11)$$

On the other hand, (3.9) and (2.3a) lead to

$$\|p\|_Q \leq \frac{1}{\beta} \|B^*(p)\|_{\mathbf{V}} \leq \|F\|_{\mathbf{V}'} + \|\{A + C\}(\mathbf{u})\|_{\mathbf{V}'}.$$

Then, we employ again the local Lipschitz continuity of $A + C$ setting $\mathbf{v} = \mathbf{0}$ in (3.7), and appeal to the inequality (3.11). Thus we arrive at

$$\begin{aligned} \|p\|_Q &\leq \|F\|_{\mathbf{V}'} + \|\mathbf{u}\|_{\mathbf{V}} + \|\mathbf{u}\|_{\mathbf{V}}^2 \\ &\leq \|F\|_{\mathbf{V}'} + \frac{1}{\alpha} \{\|F\|_{\mathbf{V}'} + \frac{1+\alpha}{\beta} \|G\|_{Q'} + \frac{1}{\beta^2} \|G\|_{Q'}^2\} \\ &\quad + \frac{1}{\alpha^2} \{\|F\|_{\mathbf{V}'} + \frac{1+\alpha}{\beta} \|G\|_{Q'} + \frac{1}{\beta^2} \|G\|_{Q'}^2\}^2 \\ &= \frac{1}{\alpha} \{(1+\alpha)\|F\|_{\mathbf{V}'} + \frac{1+\alpha}{\beta} \|G\|_{Q'} + \frac{1}{\beta^2} \|G\|_{Q'}^2\} \\ &\quad + \frac{1}{\alpha^2} \{\|F\|_{\mathbf{V}'} + \frac{1+\alpha}{\beta} \|G\|_{Q'} + \frac{1}{\beta^2} \|G\|_{Q'}^2\}^2. \end{aligned}$$

This concludes the rest of the proof. \square

4. Mixed finite element method and robust solvability. Let \mathcal{T}_h be a regular simplicial mesh defined in a bounded Lipschitz domain Ω , consisting of tetrahedral elements (or triangular elements in two dimensions) K with diameter h_K . We define the mesh size as $h := \max\{h_K : K \in \mathcal{T}_h\}$. Given an integer $k \geq 0$ and a generic element $K \in \mathcal{T}_h$, we denote by $\mathbb{P}_k(K)$ the space of polynomials defined locally in K with a degree at most k , and denote by $\mathbb{P}_k(\mathcal{T}_h)$ its global counterpart

$$\mathbb{P}_k(\mathcal{T}_h) := \{p \in L^2(\Omega) : p|_K \in \mathbb{P}_k(K), \quad \forall K \in \mathcal{T}_h\}.$$

In addition, let $\mathbb{RT}_k(\mathcal{T}_h)$ denote the $\mathbf{H}_{\Gamma_u}(\text{div}, \Omega)$ -discrete conforming subspace defined by the Raviart–Thomas elements of order k , i.e.,

$$\mathbb{RT}_k(\mathcal{T}_h) := \{\mathbf{u} \in \mathbf{H}_{\Gamma_u}(\text{div}, \Omega) : \mathbf{u}|_K = [\mathbb{P}_k(K)]^d \oplus \widetilde{\mathbb{P}}_k(K)\mathbf{x}, \quad \mathbf{x} \in \Omega \subset \mathbb{R}^d, K \in \mathcal{T}_h\},$$

where we denote by $\widetilde{\mathbb{P}}_k(K)$ the space of all polynomials over K of degree exactly equal to k and ' \oplus ' denotes the direct sum of spaces. With this we define the discrete weighted space for the velocity as follows

$$\mathbf{V} \supseteq \mathbf{V}_h := \kappa^{-\frac{1}{2}} \mathbf{L}_h^2(\Omega) \cap \mathbf{H}_{h,\Gamma_u}(\text{div}, \Omega) \cap F^{\frac{1}{3}} \mathbf{L}_h^3(\Omega), \quad (4.1)$$

where $\mathbf{L}_h^2(\Omega)$, $\mathbf{H}_{h,\Gamma_u}(\text{div}, \Omega)$, and $\mathbf{L}_h^3(\Omega)$ correspond to functions in $\mathbb{RT}_k(\mathcal{T}_h)$ equipped with the $L^2(\Omega)$, $\mathbf{H}(\text{div}, \Omega)$, and $\mathbf{L}^3(\Omega)$ -norms, respectively.

In turn, define the discrete gradient operator $\nabla_h : \mathbb{P}_k(\mathcal{T}_h) \rightarrow \mathbb{RT}_k(\mathcal{T}_h)$ by (c.f., [2, eqn. (3.1)])

$$(\nabla_h q_h, \mathbf{v}_h) = -(\text{div } \mathbf{v}_h, q_h), \quad \forall q_h \in \mathbb{P}_k(\mathcal{T}_h), \text{ and } \forall \mathbf{v}_h \in \mathbb{RT}_k(\mathcal{T}_h). \quad (4.2)$$

Additionally, define the following broken Sobolev spaces

$$\begin{aligned} H^1(\mathcal{T}_h) &:= \{p \in L^2(\Omega) : p|_K \in H^1(K), \quad \forall K \in \mathcal{T}_h\}, \\ W^{1,\frac{3}{2}}(\mathcal{T}_h) &:= \{p \in L^2(\Omega) : p|_K \in W^{1,\frac{3}{2}}(K), \quad \forall K \in \mathcal{T}_h\}, \end{aligned}$$

and whenever needed we add a subscript Γ_i denoting the part on the boundary where the value of the function is prescribed to zero. These spaces are equipped with broken Sobolev seminorms $|\bullet|_{1,\mathcal{T}_h}$ and $|\bullet|_{1,\frac{3}{2},\mathcal{T}_h}$, defined as

$$\begin{aligned} H^1(\mathcal{T}_h) \ni \zeta &\mapsto |\zeta|_{1,\mathcal{T}_h} := \left(\sum_{K \in \mathcal{T}_h} \int_K |\nabla \zeta|^2 \right)^{\frac{1}{2}}, \\ W^{1,\frac{3}{2}}(\mathcal{T}_h) \ni \xi &\mapsto |\xi|_{1,\frac{3}{2},\mathcal{T}_h} := \left(\sum_{K \in \mathcal{T}_h} \int_K |\nabla \xi|^{\frac{3}{2}} \right)^{\frac{2}{3}}, \end{aligned}$$

respectively.

Furthermore, we define the following weighted space for pressure, which is a sum of the infinite-dimensional (but broken) spaces $L^2(\Omega)$, $H_{\Gamma_p}^1(\mathcal{T}_h)$ and $W_{\Gamma_p}^{1,\frac{3}{2}}(\mathcal{T}_h)$:

$$\widehat{Q}(\mathcal{T}_h) := L^2(\Omega) + \kappa^{\frac{1}{2}} H_{\Gamma_p}^1(\mathcal{T}_h) + F^{-\frac{1}{3}} W_{\Gamma_p}^{1,\frac{3}{2}}(\mathcal{T}_h). \quad (4.3)$$

In this space we define a broken weighted norm for any $q \in \widehat{Q}(\mathcal{T}_h)$ as follows

$$\|q\|_{\widehat{Q}(\mathcal{T}_h)} := \inf_{\substack{q=q_1+q_2+q_3 \\ (q_1, q_2, q_3) \in \\ L^2(\Omega) \times H_{\Gamma_p}^1(\mathcal{T}_h) \times W_{\Gamma_p}^{1,\frac{3}{2}}(\mathcal{T}_h)}} \left(\|q_1\|_{0,\Omega} + \kappa^{\frac{1}{2}} |q_2|_{1,\mathcal{T}_h} + F^{-\frac{1}{3}} |q_3|_{1,\frac{3}{2},\mathcal{T}_h} \right).$$

Finally, we define a discrete pressure space as

$$Q_h := \kappa^{\frac{1}{2}} H_{h,\Gamma_p}^1(\Omega) + L_h^2(\Omega) + F^{-\frac{1}{3}} W_{h,\Gamma_p}^{1,\frac{3}{2}}(\Omega), \quad (4.4)$$

where $L_h^2(\Omega)$, $H_{h,\Gamma_p}^1(\Omega)$, and $W_{h,\Gamma_p}^{1,\frac{3}{2}}(\Omega)$ are polynomial spaces having discrete functions from $\mathbb{P}_k(\mathcal{T}_h)$, and equipped with the $L^2(\Omega)$ norm and the broken $H^1(\mathcal{T}_h)$, $W^{1,\frac{3}{2}}(\mathcal{T}_h)$ seminorms, respectively.

REMARK 4.1. We equip Q_h with the $\|\bullet\|_{\widehat{Q}(\mathcal{T}_h)}$ norm, and observe that $Q_h \subseteq \widehat{Q}(\mathcal{T}_h)$, but Q_h is not a subspace of Q . This entails a non-conforming (in the pressure) scheme, requiring to define a discrete bilinear form associated with the discrete divergence operator $b_h : \mathbf{V}_h \times Q_h \rightarrow \mathbb{R}$ as well as a discrete linear functional $G_h : Q_h \rightarrow \mathbb{R}$, as follows

$$b_h(\mathbf{v}_h, q_h) := \int_{\Omega} \operatorname{div} \mathbf{v}_h q_h, \quad G_h(q_h) := \int_{\Omega} g q_h, \quad \forall \mathbf{v}_h \in \mathbf{V}_h, q_h \in Q_h.$$

Then, with the conforming velocity and non-conforming pressure FE spaces (4.1) and (4.4), the mixed finite element formulation of (2.2) consists in finding $(\mathbf{u}_h, p_h) \in \mathbf{V}_h \times Q_h$ such that

$$a(\mathbf{u}_h, \mathbf{v}_h) + c(\mathbf{u}_h; \mathbf{u}_h, \mathbf{v}_h) + b_h(\mathbf{v}_h, p_h) = F(\mathbf{v}_h) \quad \forall \mathbf{v}_h \in \mathbf{V}_h, \quad (4.5a)$$

$$b_h(\mathbf{u}_h, q_h) = G_h(q_h) \quad \forall q_h \in Q_h. \quad (4.5b)$$

Similarly to the continuous case, an analysis using $\mathbf{V}_h = (\mathbb{RT}_k(\mathcal{T}_h), \|\bullet\|_{\mathbf{H}^3(\operatorname{div}, \Omega)})$ and $Q_h = (\mathbb{P}_k(\mathcal{T}_h), \|\bullet\|_{L^2(\Omega)})$ can be performed (using, e.g., [12, Theorem 4.1], [31, Theorem 3.5]) however the coercivity on the kernel and inf-sup conditions (and therefore also the stability estimates) are not necessarily robust in κ, F . To achieve such robustness we employ the weighted spaces (4.1) and (4.4).

4.1. Robust discrete solvability. First, we prove the discrete inf-sup condition, which is an essential ingredient of the proof of the parameter-robust unique solvability Theorem, discussed in this subsection. We adapt the same framework as in the continuous case to the present scenario.

LEMMA 4.1. There exists an operator \mathcal{S}_d satisfying the following properties:

$$\begin{aligned} \mathcal{S}_d \in \mathcal{L}(Q'_h, \mathbf{V}_h), \quad \|\mathcal{S}_d\|_{\mathcal{L}(Q'_h, \mathbf{V}_h)} &\text{ is independent of } \kappa, F, h \quad \text{and} \\ (\operatorname{div}[\mathcal{S}_d(g_h)], \psi_h) &= \langle g_h, \psi_h \rangle \quad \text{for all } g_h \in Q'_h, \psi_h \in Q_h. \end{aligned} \quad (4.6)$$

Proof. We first define a bounded linear operator \mathcal{S}_d from three different spaces, and then, invoke the duality relations between sum and intersection between Banach spaces (2.1) to conclude $\mathcal{S}_d \in \mathcal{L}(Q'_h, \mathbf{V}_h)$.

For the existence of $\mathcal{S}_d \in \mathcal{L}((W_{h,\Gamma_p}^{1,q}(\Omega))', \mathbf{L}_h^r(\Omega))$ with $q \in \{2, \frac{3}{2}\}$, let $\phi_h \in W_{h,\Gamma_p}^{1,r}(\Omega)$ for a given $g_h \in (W_{h,\Gamma_p}^{1,q}(\Omega))'$ with $\frac{1}{q} + \frac{1}{r} = 1$ be a unique solution of the following weak formulation

$$\langle \nabla_h \phi_h, \nabla_h \psi_h \rangle = \langle g_h, \psi_h \rangle \quad \forall \psi_h \in W_{h,\Gamma_p}^{1,q}(\Omega), \quad (4.7)$$

owing to the Banach–Nečas–Babuška theorem for elliptic problems in Banach spaces [13]. Then, it suffices to define $\mathcal{S}_d(g_h) := \nabla_h \phi_h$, where $\nabla_h \phi_h \in \mathbf{L}_h^r(\Omega)$. The continuous dependence on data coming from (4.7) also implies that $\|\mathcal{S}_d(g_h)\|_{0,r;\Omega} \lesssim \|g_h\|$. This,

in turn, shows $\mathcal{S}_d \in \mathcal{L}((W_{h,\Gamma_p}^{1,q}(\Omega))', \mathbf{L}_h^r(\Omega))$, for $q = 2$ and $q = \frac{3}{2}$ corresponding to $r = 2$ and 3 , respectively.

Next, the existence and boundedness of $\mathcal{S}_d \in \mathcal{L}((L_h^2(\Omega))', \mathbf{H}_{h,\Gamma_u}(\text{div}, \Omega))$ is a direct consequence of the surjectivity of the divergence operator from $\mathbf{H}_{\Gamma_u}(\text{div}, \Omega)$ onto $L^2(\Omega)$ and standard properties of the Raviart–Thomas interpolation (even in the case of mixed boundary conditions) [7, 16]. \square

Below, we prove the discrete inf-sup condition.

LEMMA 4.2 (Discrete inf-sup condition). *There exists a positive constant β_d , independent of h, κ and F such that*

$$\|q_h\|_{\widehat{Q}(\mathcal{T}_h)} \leq \beta_d \sup_{\mathbf{v}_h \in \mathbf{V}_h} \frac{(q_h, \text{div } \mathbf{v}_h)}{\|\mathbf{v}_h\|_{\mathbf{V}}}.$$

Proof. As a consequence of Lemma 4.1, we can assert that

$$\begin{aligned} \sup_{\mathbf{v} \neq \mathbf{v}_h \in \mathbf{V}_h} \frac{(\text{div } \mathbf{v}_h, p_h)}{\|\mathbf{v}_h\|_{\mathbf{V}}} &\geq \sup_{g_h \in Q'_h} \frac{(\text{div}[\mathcal{S}_d(g_h)], p_h)}{\|\mathcal{S}_d(g_h)\|_{\mathbf{V}}} = \sup_{g_h \in Q'_h} \frac{\langle g_h, p_h \rangle}{\|\mathcal{S}_d(g_h)\|_{\mathbf{V}}} \\ &\geq \|\mathcal{S}_d\|_{\mathcal{L}(Q'_h, \mathbf{V}_h)}^{-1} \sup_{g_h \in Q'_h} \frac{\langle g_h, p_h \rangle}{\|g_h\|_{Q'_h}} = \beta_d \|p_h\|_{\widehat{Q}(\mathcal{T}_h)}, \end{aligned}$$

which concludes the proof. \square

The following result is on robust well-posedness of the discrete mixed problem (4.5).

THEOREM 4.3 (Parameter-robust unique solvability). *Consider the weighted spaces defined in (4.1) and (4.4) with the corresponding weighted norms, and assume that $\mathbf{f} \in \mathbf{L}^2(\Omega)$, $g \in L^2(\Omega)$. Then, there exists a unique pair $(\mathbf{u}_h, p_h) \in \mathbf{V}_h \times Q_h$ of solutions to the discrete problem (4.5). Furthermore, there exists a positive constant \hat{C} independent of h , and the model parameters κ, F , such that*

$$\|(\mathbf{u}_h, q_h)\|_{\mathbf{V} \times \widehat{Q}(\mathcal{T}_h)} \leq \hat{C} \max\{\|\mathbf{f}\|_{0,\Omega} + \|g\|_{0,\Omega} + \|g\|_{0,\Omega}^2, (\|\mathbf{f}\|_{0,\Omega} + \|g\|_{0,\Omega} + \|g\|_{0,\Omega}^2)^2\}. \quad (4.8)$$

Proof. The discrete well-posedness analysis will use the discrete version of Theorem 3.1, detailed in [12, Theorem 4.1]. The local Lipschitz continuity of the discrete counterpart of $\{A + C\}$ follows similarly as in Theorem 3.3, and the discrete inf-sup condition follows from Lemma 4.2. Hence, to complete the rest of the proof, it is enough to prove the uniformly strong monotonicity.

Uniformly strong monotonicity of $\{a(\bullet, \bullet) + c(\bullet; \bullet, \bullet)\}(\bullet + \mathbf{w}_h)$. We start with the observation that since $\text{div } \mathbf{V}_h \subset Q_h$, for all $\mathbf{u}_h \in \mathbf{Z}_h := \{\mathbf{v}_h \in \mathbf{V}_h : b_h(\mathbf{v}_h, q_h) = 0 \quad \forall q_h \in Q_h\}$, we can choose $q_h = \text{div } \mathbf{u}_h \in Q_h$. Therefore, we characterise the discrete kernel as follows

$$\mathbf{Z}_h = \{\mathbf{v}_h \in \mathbf{V}_h : \text{div } \mathbf{v}_h = 0\},$$

and we remark that $\mathbf{Z}_h \subseteq \mathbf{Z}$, which directly follows from the characterisation of \mathbf{Z}_h . Now, for $\mathbf{u}_h, \mathbf{v}_h \in \mathbf{Z}_h$ and $\mathbf{w}_h \in \mathbf{V}_h$, the following relation holds

$$\begin{aligned} &a(\mathbf{u}_h + \mathbf{w}_h, \mathbf{u}_h - \mathbf{v}_h) + c(\mathbf{u}_h + \mathbf{w}_h; \mathbf{u}_h + \mathbf{w}_h, \mathbf{u}_h - \mathbf{v}_h) - a(\mathbf{v}_h + \mathbf{w}_h, \mathbf{u}_h - \mathbf{v}_h) - \\ &c(\mathbf{v}_h + \mathbf{w}_h; \mathbf{v}_h + \mathbf{w}_h, \mathbf{u}_h - \mathbf{v}_h) \\ &= \int_{\Omega} \kappa^{-1} |\mathbf{u}_h - \mathbf{v}_h|^2 + F \int_{\Omega} ((\mathbf{u}_h + \mathbf{w}_h)|\mathbf{u}_h + \mathbf{w}_h| - (\mathbf{v}_h + \mathbf{w}_h)|\mathbf{v}_h + \mathbf{w}_h|) \cdot (\mathbf{u}_h - \mathbf{v}_h). \end{aligned}$$

By employing [6, Lemma 2.1, equation (2.1b)] we deduce that there exists a constant $\hat{C} > 0$ independent of h, κ , and F , such that

$$F \int_{\Omega} ((\mathbf{u}_h + \mathbf{w}_h)|\mathbf{u}_h + \mathbf{w}_h| - (\mathbf{v}_h + \mathbf{w}_h)|\mathbf{v}_h + \mathbf{w}_h|) \cdot (\mathbf{u}_h - \mathbf{v}_h) \geq \hat{C} F \|\mathbf{u}_h - \mathbf{v}_h\|_{0,3,\Omega}^3.$$

Finally, setting $\tilde{\alpha}^{\frac{1}{2}} = \min\{1, \hat{C}^{\frac{1}{3}}\}$, there holds

$$\begin{aligned} & a(\mathbf{u}_h + \mathbf{w}_h, \mathbf{u}_h - \mathbf{v}_h) + c(\mathbf{u}_h + \mathbf{w}_h; \mathbf{u}_h + \mathbf{w}_h, \mathbf{u}_h - \mathbf{v}_h) \\ & - a(\mathbf{v}_h + \mathbf{w}_h, \mathbf{u}_h - \mathbf{v}_h) - c(\mathbf{v}_h + \mathbf{w}_h; \mathbf{v}_h + \mathbf{w}_h, \mathbf{u}_h - \mathbf{v}_h) \geq \tilde{\alpha} \|\mathbf{u}_h - \mathbf{v}_h\|_{\mathbf{V}}^2, \end{aligned} \quad (4.9)$$

where we have used that the $\mathbf{H}(\text{div})$ -seminorm is zero since $\mathbf{u}_h, \mathbf{v}_h \in \mathbf{Z}_h$. Note also that $\tilde{\alpha}$ is independent of h, κ , and F .

Thus, an appeal to the discrete version of the Theorem 3.1 ensures existence and uniqueness of the discrete solution. Finally, the discrete stability estimate (4.8) follows similarly to the continuous case (Theorem 3.3), and we observe that the discrete stability constant is independent of h, κ , and F . \square

4.2. A priori error analysis. In this section, we estimate the error between the exact and approximate solutions, showing that the convergence is robust in the material parameters.

Below, we prove a theorem on *a priori* error estimate for the Darcy–Forchheimer model, which are robust with respect to κ, h , and F .

THEOREM 4.4 (Quasi-optimality). *Let (\mathbf{u}, p) uniquely solve the continuous model (2.3), and let the pair (\mathbf{u}_h, p_h) be the solution of the discrete model (4.5). Then, the following quasi-optimal error estimates for the velocity and pressure hold*

$$\|\mathbf{u} - \mathbf{u}_h\|_{\mathbf{V}} + \|p - p_h\|_{\tilde{Q}(\mathcal{T}_h)} \leq C_c (\text{dist}(\mathbf{u}, \mathbf{V}_h) + \text{dist}(p, Q_h)), \quad (4.10)$$

where C_c is independent of h, κ and F .

Proof. Now, define

$$\mathbf{Z}_h^g := \{\mathbf{v}_h \in \mathbf{V}_h : b_h(\mathbf{v}_h, q_h) = G(q_h) \quad \forall q_h \in Q_h\}. \quad (4.11)$$

Note that $\mathbf{u}_h \in \mathbf{Z}_h^g$ and $\mathbf{u}_h - \mathbf{u}_h^g \in \mathbf{Z}_h$ for all $\mathbf{u}_h^g \in \mathbf{Z}_h^g$. From triangle inequality, an application of uniformly strong monotonicity of $a(\bullet, \bullet) + c(\bullet, \bullet, \bullet)$ to the pair $(\mathbf{u}_h - \mathbf{u}_h^g, \mathbf{0}) \in \mathbf{Z}_h \times \mathbf{Z}_h$, and choosing $\mathbf{w}_h = \mathbf{u}_h^g$ in (4.9), we arrive at

$$\tilde{\alpha} \|\mathbf{u}_h - \mathbf{u}_h^g\|_{\mathbf{V}}^2 \leq a(\mathbf{u}_h, \mathbf{u}_h - \mathbf{u}_h^g) + c(\mathbf{u}_h; \mathbf{u}_h, \mathbf{u}_h) - a(\mathbf{u}_h^g, \mathbf{u}_h - \mathbf{u}_h^g) - c(\mathbf{u}_h^g, \mathbf{u}_h - \mathbf{u}_h^g).$$

Further, adding and subtracting $a(\mathbf{u}, \mathbf{u}_h - \mathbf{u}_h^g) + c(\mathbf{u}; \mathbf{u}, \mathbf{u}_h - \mathbf{u}_h^g)$ to the right-hand side of the above inequality, the following bound is obtained

$$\begin{aligned} \tilde{\alpha} \|\mathbf{u}_h - \mathbf{u}_h^g\|_{\mathbf{V}}^2 &\leq a(\mathbf{u}, \mathbf{u}_h - \mathbf{u}_h^g) + c(\mathbf{u}; \mathbf{u}, \mathbf{u}_h - \mathbf{u}_h^g) - a(\mathbf{u}_h^g, \mathbf{u}_h - \mathbf{u}_h^g) \\ &\quad - c(\mathbf{u}_h^g; \mathbf{u}_h^g, \mathbf{u}_h - \mathbf{u}_h^g) + a(\mathbf{u}_h, \mathbf{u}_h - \mathbf{u}_h^g) + c(\mathbf{u}_h; \mathbf{u}_h, \mathbf{u}_h - \mathbf{u}_h^g) \\ &\quad - a(\mathbf{u}, \mathbf{u}_h - \mathbf{u}_h^g) - c(\mathbf{u}; \mathbf{u}, \mathbf{u}_h - \mathbf{u}_h^g). \end{aligned} \quad (4.12)$$

Next, from (4.5a), we observe that

$$\begin{aligned} & a(\mathbf{u}, \mathbf{u}_h - \mathbf{u}_h^g) + c(\mathbf{u}; \mathbf{u}, \mathbf{u}_h - \mathbf{u}_h^g) - a(\mathbf{u}_h, \mathbf{u}_h - \mathbf{u}_h^g) - c(\mathbf{u}_h; \mathbf{u}_h, \mathbf{u}_h - \mathbf{u}_h^g) \\ & = b_h(\mathbf{u}_h - \mathbf{u}_h^g, p - p_h). \end{aligned} \quad (4.13)$$

Then, combining (4.12), (4.13), the local Lipschitz continuity of $a(\bullet, \bullet) + c(\bullet; \bullet, \bullet)$, and the boundedness of $b_h(\bullet, \bullet)$, we arrive at

$$\tilde{\alpha} \|\mathbf{u}_h - \mathbf{u}_h^g\|_{\mathbf{v}} \leq \|p - p_h\|_{\hat{Q}(\mathcal{T}_h)} + (1 + \|\mathbf{u}\|_{\mathbf{v}} + \|\mathbf{u}_h^g\|_{\mathbf{v}}) \|\mathbf{u} - \mathbf{u}_h^g\|_{\mathbf{v}}.$$

Finally, a use of the triangle inequality yields the estimate for the velocity error as

$$\begin{aligned} \|\mathbf{u} - \mathbf{u}_h\|_{\mathbf{v}} &\leq \frac{1}{\tilde{\alpha}} \|p - p_h\|_{\hat{Q}(\mathcal{T}_h)} + \frac{1}{\tilde{\alpha}} ((1 + \tilde{\alpha}) + \|\mathbf{u}\|_{\mathbf{v}} + \|\mathbf{u}_h^g\|_{\mathbf{v}}) \|\mathbf{u} - \mathbf{u}_h^g\|_{\mathbf{v}} \\ &\leq C_g (\text{dist}(p, Q_h) + \text{dist}(\mathbf{u}, \mathbf{V}_h)), \end{aligned} \quad (4.14)$$

where $C_g := \max\{\frac{1}{\tilde{\alpha}}, \frac{1}{\tilde{\alpha}}(1 + \frac{1}{\beta_d})((1 + \tilde{\alpha}) + \|\mathbf{u}\|_{\mathbf{v}} + \|\mathbf{u}_h^g\|_{\mathbf{v}})\}$, which is obtained by using that $\text{dist}(\mathbf{u}, \mathbf{Z}_h^g) \leq (1 + \frac{1}{\beta_d}) \text{dist}(\mathbf{u}, \mathbf{V}_h)$ (see for instance, [16, Theorem 2.6]).

Now, for the pressure estimate, we use the inf-sup stability of $b_h(\bullet, \bullet)$. Let $p_h^* \in Q_h$ be an arbitrary element. Then, there holds

$$\begin{aligned} \beta_d \|p_h - p_h^*\|_{\hat{Q}(\mathcal{T}_h)} &\leq \sup_{\mathbf{0} \neq \mathbf{v}_h \in \mathbf{V}_h} \frac{b_h(\mathbf{v}_h, p_h - p_h^*)}{\|\mathbf{v}_h\|_{\mathbf{v}}} \\ &= \sup_{\mathbf{0} \neq \mathbf{v}_h \in \mathbf{V}_h} \frac{b_h(\mathbf{v}_h, p - p_h^*) + b_h(\mathbf{v}_h, p_h - p)}{\|\mathbf{v}_h\|_{\mathbf{v}}} \\ &= \sup_{\mathbf{0} \neq \mathbf{v}_h \in \mathbf{V}_h} \frac{b_h(\mathbf{v}_h, p - p_h^*) + a(\mathbf{u}_h - \mathbf{u}, p - p_h)}{\|\mathbf{v}_h\|_{\mathbf{v}}} \\ &\leq \|p - p_h^*\|_{\hat{Q}(\mathcal{T}_h)} + (1 + \|\mathbf{u}\|_{\mathbf{v}} + \|\mathbf{u}_h^g\|_{\mathbf{v}}) \|\mathbf{u} - \mathbf{u}_h\|_{\mathbf{v}}, \end{aligned}$$

which upon using the triangle inequality, shows the following estimate on the pressure

$$\|p - p_h\|_{\hat{Q}(\mathcal{T}_h)} \leq \tilde{C}_g (\text{dist}(p, Q_h) + \text{dist}(\mathbf{u}, \mathbf{V}_h)), \quad (4.15)$$

where $\tilde{C}_g := \max\{(1 + \frac{1}{\beta_d}) + C_g^{\frac{1}{2}}(1 + \|\mathbf{u}\|_{\mathbf{v}} + \|\mathbf{u}_h^g\|_{\mathbf{v}}), C_g^{\frac{1}{2}}(1 + \|\mathbf{u}\|_{\mathbf{v}} + \|\mathbf{u}_h^g\|_{\mathbf{v}})\}$. This concludes the proof. \square

Additionally, if $\mathbf{Z}_h \subseteq \mathbf{Z}$, then, we obtain the following pressure-independent estimate (cf. [16, Theorem B.2]) for the velocity.

COROLLARY 4.5. *Under the assumptions of Theorem 4.4, there holds for any $\mathbf{u}_h^g \in \mathbf{Z}_h^g$*

$$\|\mathbf{u} - \mathbf{u}_h\|_{\mathbf{v}} \leq C_D \text{dist}(\mathbf{u}, \mathbf{V}_h), \quad (4.16)$$

where $C_D := \frac{1}{\tilde{\alpha}}((1 + \tilde{\alpha}) + \|\mathbf{u}\|_{\mathbf{v}} + \|\mathbf{u}_h^g\|_{\mathbf{v}})(1 + \frac{1}{\beta_d}) > 0$ is independent of h, κ , and F .

Proof. From the characterisation of \mathbf{Z}_h , there holds $b_h(\mathbf{v}_h, q - q_h) = 0$ for all $\mathbf{v}_h \in \mathbf{Z}_h$. Then, from (4.5b), it is evident that $\mathbf{u}_h \in \mathbf{Z}_h^g$. Now, let \mathbf{u}_h^g be an arbitrary, but fixed element in \mathbf{Z}_h^g , then $\mathbf{u}_h - \mathbf{u}_h^g \in \mathbf{Z}_h$. A use of the triangle inequality shows

$$\|\mathbf{u} - \mathbf{u}_h\|_{\mathbf{v}} \leq \|\mathbf{u} - \mathbf{u}_h^g\|_{\mathbf{v}} + \|\mathbf{u}_h - \mathbf{u}_h^g\|_{\mathbf{v}}.$$

Apply the uniformly strong monotonicity of $a(\bullet, \bullet) + c(\bullet; \bullet, \bullet)$ to the pair $(\mathbf{u}_h - \mathbf{u}_h^g, \mathbf{0}) \in \mathbf{Z}_h \times \mathbf{Z}_h$ and also take $\mathbf{w}_h = \mathbf{u}_h^g$ in (4.9) to arrive at

$$\begin{aligned} \tilde{\alpha} \|\mathbf{u}_h - \mathbf{u}_h^g\|_{\mathbf{v}}^2 &= a(\mathbf{u}_h - \mathbf{u}_h^g - \mathbf{u}_h^g, \mathbf{u}_h - \mathbf{u}_h^g) + c(\mathbf{u}_h - \mathbf{u}_h^g + \mathbf{u}_h^g; \mathbf{u}_h - \mathbf{u}_h^g + \mathbf{u}_h^g, \mathbf{u}_h - \mathbf{u}_h^g) \\ &\quad - a(\mathbf{u}_h^g, \mathbf{u}_h - \mathbf{u}_h^g) - c(\mathbf{u}_h^g; \mathbf{u}_h^g, \mathbf{u}_h - \mathbf{u}_h^g) \end{aligned} \quad (4.17)$$

$$= a(\mathbf{u}_h, \mathbf{u}_h - \mathbf{u}_h^g) + c(\mathbf{u}_h; \mathbf{u}_h, \mathbf{u}_h - \mathbf{u}_h^g) - a(\mathbf{u}_h^g, \mathbf{u}_h - \mathbf{u}_h^g) - c(\mathbf{u}_h^g; \mathbf{u}_h^g, \mathbf{u}_h - \mathbf{u}_h^g).$$

Observe that, by adding and subtracting $a(\mathbf{u}, \mathbf{u}_h - \mathbf{u}_h^g) + c(\mathbf{u}; \mathbf{u}, \mathbf{u}_h - \mathbf{u}_h^g)$ on the right-hand side of (4.17), and using (2.3a) and (4.5a), as well as the fact that $b_h(\mathbf{u}_h - \mathbf{u}_h^g, q_h) = 0$ for all $q_h \in Q_h$, we deduce the following:

$$\begin{aligned} & \tilde{\alpha} \|\mathbf{u}_h - \mathbf{u}_h^g\|_{\mathbf{V}} \\ & \leq b_h(\mathbf{u}_h, \mathbf{u}_h^g, p - p_h) + a(\mathbf{u}, \mathbf{u}_h - \mathbf{u}_h^g) + c(\mathbf{u}; \mathbf{u}, \mathbf{u}_h - \mathbf{u}_h^g) - a(\mathbf{u}_h^g, \mathbf{u}_h - \mathbf{u}_h^g) \\ & \quad - c(\mathbf{u}_h^g; \mathbf{u}_h^g, \mathbf{u}_h - \mathbf{u}_h^g) \\ & = a(\mathbf{u}, \mathbf{u}_h - \mathbf{u}_h^g) + c(\mathbf{u}; \mathbf{u}, \mathbf{u}_h - \mathbf{u}_h^g) - a(\mathbf{u}_h^g, \mathbf{u}_h - \mathbf{u}_h^g) - c(\mathbf{u}_h^g; \mathbf{u}_h^g, \mathbf{u}_h - \mathbf{u}_h^g) \\ & \leq (1 + \|\mathbf{u}\|_{\mathbf{V}} + \|\mathbf{u}_h^g\|_{\mathbf{V}}) \|\mathbf{u} - \mathbf{u}_h^g\|_{\mathbf{V}}, \end{aligned}$$

where we have used that $\mathbf{Z}_h \subseteq \mathbf{Z}$ in the second step, and the local Lipschitz property of $a(\bullet, \bullet) + c(\bullet; \bullet, \bullet)$ in the third step. Finally, a use of the triangle inequality yields

$$\|\mathbf{u} - \mathbf{u}_h\|_{\mathbf{V}} \leq \frac{1}{\tilde{\alpha}} ((1 + \tilde{\alpha}) + \|\mathbf{u}\|_{\mathbf{V}} + \|\mathbf{u}_h^g\|_{\mathbf{V}}) \text{dist}(\mathbf{u}, \mathbf{Z}_h^g).$$

Recalling from [16, Theorem 2.6] that $\text{dist}(\mathbf{u}, \mathbf{Z}_h^g) \leq (1 + \frac{1}{\beta_d}) \text{dist}(\mathbf{u}, \mathbf{V}_h)$, where β_d is the discrete inf-sup constant, we achieve the desired pressure-robustness. \square

Let us remark that by just considering the spaces $\mathbf{H}_{\Gamma_u}^3(\text{div}, \Omega)$ for the velocity and $L^2(\Omega)$ for the pressure and following the approach of [31] one can obtain the pressure and velocity error estimates separately, but they are not necessarily robust with respect to the parameters κ, F .

In order to provide a theoretical rate of convergence for the mixed FEM (4.5), we recall the approximation properties of the subspaces involved.

(**AP** $_h^{\mathbf{u}}$). For the Fortin operator $\Pi_h : \mathbf{W}^{m,r}(\Omega) \cap \mathbf{H}^l(\text{div}, \Omega) \rightarrow \mathbb{RT}_k(\mathcal{T}_h)$, $0 \leq m \leq l$, $1 \leq l \leq k+1$ (see [17, 7, 31]), there holds:

$$\begin{aligned} & \star \|\Pi_h \mathbf{v} - \mathbf{v}\|_{m,r,\Omega} \leq \hat{C} h^{l-m} \|\mathbf{v}\|_{l,r,\Omega} \quad \forall \mathbf{v} \in \mathbf{W}^{m,r}(\Omega), 0 \leq m \leq l, 1 \leq l \leq k+1, \\ & \star \|\text{div}(\Pi_h \mathbf{v} - \mathbf{v})\|_{0,\Omega} \leq \hat{C} h^l \|\text{div } \mathbf{v}\|_{l,\Omega} \quad \forall \mathbf{v} \in \mathbf{H}^l(\text{div}, \Omega), 0 \leq l \leq k+1, \end{aligned}$$

where $\hat{C} > 0$ is independent of h .

(**AP** $_h^p$). Let $P_h : W^{l,r}(K) \rightarrow \mathbb{P}_k(\mathcal{T}_h)$, $0 \leq m \leq l$, $0 \leq l \leq k+1$, be the orthogonal L^2 projection. Then, there exists a positive constant $C_{\sharp} > 0$, independent of h , satisfying (see, [13])

$$\star |P_h q - q|_{m,r,K} \leq C_{\sharp} h^{l-m} |p|_{l,r,K} \quad \forall q \in W^{l,r}(K), K \in \mathcal{T}_h, 0 \leq m \leq l, 0 \leq l \leq k+1.$$

To conclude this section, the following theorem provides the theoretical rate of convergence of the mixed finite element Galerkin scheme (2.3), under suitable regularity assumptions on the exact solution.

THEOREM 4.6 (Convergence rates). *Let $(\mathbf{u}, p) \in \mathbf{V} \times Q$ be the solution of the continuous problem (2.3) with the following regularity conditions:*

$$\begin{aligned} & \mathbf{u} \in \kappa^{-\frac{1}{2}} \mathbf{H}^{l+1}(\Omega) \cap \mathbf{F}^{\frac{1}{3}} \mathbf{W}^{l+1,3}(\Omega), \quad \text{div } \mathbf{u} \in H^{l+1}(\Omega), \\ & \text{and} \quad p \in \kappa^{\frac{1}{2}} H^{l+2}(\Omega) \cap \mathbf{F}^{-\frac{1}{3}} \mathbf{W}^{l+2,\frac{3}{2}}(\Omega), \end{aligned}$$

where $0 \leq l \leq k+1$. Then, there exists a positive constant $C_b > 0$, independent of h, κ , and \mathbf{F} , such that

$$\begin{aligned} \|\mathbf{u} - \mathbf{u}_h\|_{\mathbf{V}} + \|p - p_h\|_{\widehat{\mathbf{Q}}(\mathcal{T}_h)} &\leq C_b h^{l+1} \left\{ \kappa^{-\frac{1}{2}} \|\mathbf{u}\|_{l+1,\Omega} + \|\operatorname{div} \mathbf{u}\|_{l+1,\Omega} + \mathbf{F}^{\frac{1}{3}} \|\mathbf{u}\|_{l+1,3,\Omega} \right\} \\ &\quad + C_b h^{l+1} \left\{ |p|_{l+1,\Omega}^2 + \kappa |p|_{l+2,\Omega}^2 + \mathbf{F}^{-\frac{2}{3}} |p|_{l+2,\frac{3}{2},\Omega} \right\}^{\frac{1}{2}}. \end{aligned}$$

Proof. The proof follows directly from the quasi-optimality estimate (4.10) and the above approximation properties, in the following manner

$$\begin{aligned} \|\mathbf{u} - \mathbf{u}_h\|_{\mathbf{V}} + \|p - p_h\|_{\widehat{\mathbf{Q}}(\mathcal{T}_h)} &\leq C_c (\operatorname{dist}(\mathbf{u}, \mathbf{V}_h) + \operatorname{dist}(p, \mathbf{Q}_h)) \\ &\leq \widetilde{C}_c (\|\mathbf{u} - \widetilde{\Pi}_h(\mathbf{u})\|_{\mathbf{V}} + \|p - \widetilde{P}_h(p)\|_{\widehat{\mathbf{Q}}(\mathcal{T}_h)}) \\ &\leq C_b h^{l+1} \left\{ \kappa^{-\frac{1}{2}} \|\mathbf{u}\|_{l+1,\Omega} + \|\operatorname{div} \mathbf{u}\|_{l+1,\Omega} + \mathbf{F}^{\frac{1}{3}} \|\mathbf{u}\|_{l+1,3,\Omega} \right\} \\ &\quad + C_b h^{l+1} \left\{ |p|_{l+1,\Omega}^2 + \kappa |p|_{l+2,\Omega}^2 + \mathbf{F}^{-\frac{2}{3}} |p|_{l+2,\frac{3}{2},\Omega} \right\}^{\frac{1}{2}}, \end{aligned}$$

where, $\widetilde{\Pi}_h, \widetilde{P}_h$ are scaled (with suitable constants independent of h, κ, \mathbf{F}) counterparts of Π_h and P_h , and $C_b = \widetilde{C}_c \max\{\dot{C}, C_{\sharp}\}$. This completes the rest of the proof. \square

5. Preconditioning for the linearised Darcy–Forchheimer equations. In this section, we define a variable operator preconditioner for the Newton linearisation of (2.3). Using the notation from Section 3, we first rewrite such system in operator form as

$$\begin{pmatrix} A + C & B^* \\ B & 0 \end{pmatrix} \begin{pmatrix} \mathbf{u} \\ p \end{pmatrix} = \begin{pmatrix} F \\ G \end{pmatrix} \quad \text{in } \mathbf{V}' \times \mathbf{Q}'. \quad (5.1)$$

Let us denote by $\mathcal{H}(\mathbf{u})$ the Gâteaux derivative of the nonlinear operator C , i.e., $|\mathbf{u}|^{r-2} \mathbf{u}$ at the state \mathbf{u} in the direction of $\delta \mathbf{u}$. In addition, consider now the Newton–Raphson linearisation of (5.1), which starting from an initial guess \mathbf{u}^0, p^0 , and iterating on $m = 1, \dots$ until convergence, seeks velocity and pressure increments $(\delta \mathbf{u}, \delta p)$ in a new space

$$\begin{aligned} \underline{\mathbf{V}} \times \underline{\mathbf{Q}} := & [\kappa^{-\frac{1}{2}} \mathbf{L}^2(\Omega) \cap \mathbf{H}_{\Gamma_u}(\operatorname{div}, \Omega) \cap \{\mathbf{F}\mathcal{H}(\hat{\mathbf{u}})\}^{\frac{1}{3}} \mathbf{L}^3(\Omega)] \\ & \times [\mathbf{L}^2(\Omega) + \kappa^{\frac{1}{2}} \mathbf{H}_{\Gamma_p}^1(\Omega) + \{\mathbf{F}\mathcal{H}(\hat{\mathbf{u}})\}^{-\frac{1}{3}} \mathbf{W}_{\Gamma_p}^{1, \frac{3}{2}}(\Omega)], \end{aligned} \quad (5.2)$$

such that

$$\begin{pmatrix} \kappa^{-1} \mathcal{I} + \mathbf{F}\mathcal{H}(\mathbf{u}^m) \mathcal{I} & B^* \\ B & 0 \end{pmatrix} \begin{pmatrix} \delta \mathbf{u} \\ \delta p \end{pmatrix} = \begin{pmatrix} F - \{A + C\}(\mathbf{u}^m) - B^*(p^m) \\ G - B(\mathbf{u}^m) \end{pmatrix} \quad \text{in } \underline{\mathbf{V}}' \times \underline{\mathbf{Q}}'. \quad (5.3)$$

Here, \mathcal{I} denotes the identity operator at the continuous level, but for the discrete case it stands for the corresponding mass matrix (either for velocity or pressure). Further, we note that, in weak form, the action of the operator $\mathbf{F}\mathcal{H}(\mathbf{u}^m) \mathcal{I} : \underline{\mathbf{V}} \rightarrow \underline{\mathbf{V}}'$ reads

$$\langle \mathbf{F}\mathcal{H}(\mathbf{u}^m)(\delta \mathbf{u}), \mathbf{v} \rangle = \int_{\Omega} \mathbf{F} |\mathbf{u}^m|^{r-2} \delta \mathbf{u} \cdot \mathbf{v} + \int_{\Omega} \mathbf{F}(r-2) |\mathbf{u}^m|^{r-4} (\mathbf{u}^m \cdot \delta \mathbf{u})(\mathbf{u}^m \cdot \mathbf{v}).$$

Then, update the solution as $(\mathbf{u}^{m+1}, p^{m+1}) = (\mathbf{u}^m + \delta \mathbf{u}, p^m + \delta p)$. Next Lemma is on the solvability of the system (5.3).

LEMMA 5.1. *Assume that for any $\mathbf{w} \in \underline{\mathbf{V}}$, the function $\mathbf{F}\mathcal{H}(\mathbf{w})$ is in $\mathbf{L}^\infty(\Omega)$ and that $\mathbf{F}\mathcal{H}(\mathbf{w})(\mathbf{x}) \geq 0$ a.e. in Ω . Then, the problem (5.3) has a unique solution in $\underline{\mathbf{V}} \times \underline{\mathbf{Q}}$.*

Proof. We use the classical Babuška–Brezzi theory for saddle-point problems. The bilinear form $\tilde{a} : \underline{\mathbf{V}} \times \underline{\mathbf{V}} \rightarrow \mathbb{R}$ defined as

$$\tilde{a}(\mathbf{u}, \mathbf{v}) := a(\mathbf{u}, \mathbf{v}) + \langle \mathbf{F}\mathcal{H}(\mathbf{u}^m)(\mathbf{u}), \mathbf{v} \rangle,$$

is bounded in $\underline{\mathbf{V}}$ using the Hölder’s inequality and coercive in $\underline{\mathbf{Z}} = \ker B$; all with constants independent of κ , \mathbf{F} , and $\mathcal{H}(\mathbf{u}^m)$. Finally, the boundedness and inf-sup condition on B have been shown in the proof of Theorem 3.3 for a different weight. In this case, we only need to alter the scaling, which completes the rest of the proof. \square

The spaces defined in (5.2) induce a duality map that can be used for preconditioning the system (5.3), which is discussed below.

THEOREM 5.2 (Local preconditioner for the tangent system). *Let $(\hat{\mathbf{u}}, \hat{p}) \in \underline{\mathbf{V}} \times \underline{\mathbf{Q}}$ be the state around which the Newton–Raphson linearisation is performed. Then the following block diagonal operator*

$$\begin{pmatrix} \mathcal{P} := (\kappa^{-1}\mathcal{I} + \mathbf{F}\mathcal{H}(\hat{\mathbf{u}})\mathcal{I} - \nabla \operatorname{div})^{-1} & 0 \\ 0 & \mathcal{Q} := \mathcal{I}^{-1} + (-\kappa\Delta)^{-1} - ([\mathbf{F}\mathcal{H}(\hat{\mathbf{u}})]^{-1}\Delta_{\frac{3}{2}})^{-1} \end{pmatrix}, \quad (5.4)$$

is a parameter-robust preconditioner for (5.3), in the sense that the condition numbers of the preconditioned matrix are uniformly bounded in κ and \mathbf{F} . Here, making abuse of notation, by $[\mathbf{F}\mathcal{H}(\hat{\mathbf{u}})]^{-1}\Delta_{\frac{3}{2}}$ we denote the (singular) weighted p -Laplace operator associated with the space $W_{\Gamma_p}^{1,\frac{3}{2}}(\Omega)$, defined as

$$\langle [\mathbf{F}\mathcal{H}(\hat{\mathbf{u}})]^{-1}\Delta_{\frac{3}{2}}\phi, \psi \rangle := \int_{\Omega} [\mathbf{F}\mathcal{H}(\hat{\mathbf{u}})]^{-1}|\nabla\phi|^{-\frac{1}{2}}\nabla\phi \cdot \nabla\psi, \quad \forall \psi \in W^{1,3}(\Omega).$$

Proof. Preconditioners for the upper diagonal block in system (5.3) can be directly constructed following the approach of [5, Equation 7]. This straightforwardly leads to \mathcal{P} in (5.4). We now focus on showing that \mathcal{Q} is a preconditioner for the pressure block. Observe that the norm for the space $\underline{\mathbf{Q}}$ in (5.2) can be written as

$$\|q\|_{\underline{\mathbf{Q}}}^2 := \inf_{\varphi \in H_{\Gamma_p}^1(\Omega)} \{ \|q - \varphi\|_{0,\Omega}^2 + \kappa \|\nabla\varphi\|_{0,\Omega}^2 + [\mathbf{F}\mathcal{H}(\hat{\mathbf{u}})]^{-1} \|\nabla\varphi\|_{0,\frac{3}{2},\Omega}^{\frac{3}{2}} \}. \quad (5.5)$$

Note that the above infimum is attained by a $\varphi \in H_{\Gamma_p}^1(\Omega)$ (therefore also in $L^2(\Omega)$) and $W_{\Gamma_p}^{1,\frac{3}{2}}(\Omega)$ that satisfies

$$(\mathcal{I} - \kappa\Delta - [\mathbf{F}\mathcal{H}(\hat{\mathbf{u}})]^{-1}\Delta_{\frac{3}{2}})\varphi = q \quad \text{in } \Omega, \quad (5.6a)$$

$$(\kappa\nabla\varphi + [\mathbf{F}\mathcal{H}(\hat{\mathbf{u}})]^{-1}|\nabla\varphi|^{-\frac{1}{2}}\nabla\varphi) \cdot \mathbf{n} = 0 \quad \text{on } \Gamma_{\mathbf{u}}, \quad (5.6b)$$

$$\varphi = 0 \quad \text{on } \Gamma_p. \quad (5.6c)$$

The unique solvability of (5.6) follows from the Minty–Browder framework for monotone operators, stressing that q is from a suitable dual space (following from Sobolev embedding). Further details are omitted. Using (5.6), we obtain the following

$$\begin{aligned} \|q\|_{\underline{\mathbf{Q}}}^2 &= \|q - \varphi\|_{0,\Omega}^2 + \kappa \|\nabla\varphi\|_{0,\Omega}^2 + [\mathbf{F}\mathcal{H}(\hat{\mathbf{u}})]^{-1} \|\nabla\varphi\|_{0,\frac{3}{2},\Omega}^{\frac{3}{2}} \\ &= \langle -\kappa\Delta\varphi - [\mathbf{F}\mathcal{H}(\hat{\mathbf{u}})]^{-1}\Delta_{\frac{3}{2}}\varphi, -\kappa\Delta\varphi - [\mathbf{F}\mathcal{H}(\hat{\mathbf{u}})]^{-1}\Delta_{\frac{3}{2}}\varphi \rangle - \kappa \langle \Delta\varphi, \varphi \rangle \end{aligned}$$

$$\begin{aligned}
& - \langle [\mathbf{F}\mathcal{H}(\hat{\mathbf{u}})]^{-1} \Delta_{\frac{3}{2}} \varphi, \varphi \rangle \\
& = \langle (-\kappa \Delta - [\mathbf{F}\mathcal{H}(\hat{\mathbf{u}})]^{-1} \Delta_{\frac{3}{2}}) \varphi, (\mathcal{I} - \kappa \Delta - [\mathbf{F}\mathcal{H}(\hat{\mathbf{u}})]^{-1} \Delta_{\frac{3}{2}}) \varphi \rangle.
\end{aligned}$$

Next, we employ again (5.6) to conclude that

$$\|q\|_{\underline{Q}}^2 = \langle (-\kappa \Delta - [\mathbf{F}\mathcal{H}(\hat{\mathbf{u}})]^{-1} \Delta_{\frac{3}{2}})(\mathcal{I} - \kappa \Delta - [\mathbf{F}\mathcal{H}(\hat{\mathbf{u}})]^{-1} \Delta_{\frac{3}{2}})^{-1} q, q \rangle. \quad (5.7)$$

Then, using the duality map we readily define the canonical preconditioner $\mathcal{Q} : \underline{Q}' \rightarrow \underline{Q}$ associated with (5.7) by

$$\mathcal{Q} = (\mathcal{I} - \kappa \Delta - [\mathbf{F}\mathcal{H}(\hat{\mathbf{u}})]^{-1} \Delta_{\frac{3}{2}})^{-1}.$$

Therefore, proceeding similarly as in [28, Section 3], we can assert that (5.4) is a (κ, \mathbf{F}) -robust block diagonal preconditioner for system (5.3). This concludes the proof. \square

Let us stress that it is also possible to define a simpler preconditioner (motivated by [5]) for the linearised problem (5.3) by using a Schur complement approach (following, e.g., [28, 22, 34]) involving the space

$$\underline{\underline{\mathbf{V}}} \times \underline{\underline{Q}} := (\kappa^{-1} + \mathbf{F}\mathcal{H}(\hat{\mathbf{u}}))[\mathbf{L}^2(\Omega) \cap \mathbf{H}_{\Gamma_u}(\text{div}, \Omega)] \times (\kappa^{-1} + \mathbf{F}\mathcal{H}(\hat{\mathbf{u}}))^{-1} \mathbf{L}^2(\Omega),$$

where again $(\hat{\mathbf{u}}, \hat{p}) \in \underline{\underline{\mathbf{V}}} \times \underline{\underline{Q}}$ is the state around which the Newton–Raphson linearisation is performed. This space is associated with the block diagonal Riesz map

$$\begin{pmatrix} \mathcal{P} := ([\kappa^{-1} \mathcal{I} + \mathbf{F}\mathcal{H}(\hat{\mathbf{u}})] (\mathcal{I} - \nabla \text{div}))^{-1} & 0 \\ 0 & ([\kappa^{-1} \mathcal{I} + \mathbf{F}\mathcal{H}(\hat{\mathbf{u}})]^{-1} \mathcal{I})^{-1} \end{pmatrix}. \quad (5.8)$$

The parameter-robustness for this preconditioner can be easily inferred from a scaling argument as in [28, Example 3.2]. Nevertheless this preconditioner might not be of much interest in the case of coupling with other multiphysics effects. This has been discussed in length in [5].

6. Numerical results. The purpose of this section is to experimentally validate the theoretical results presented in the previous sections. We verify that the convergence rates are robust in the proposed finite element method, and also illustrate the performance of proposed schemes in typical porous media flow problems in 2D and 3D. The numerical implementation is based on the open-source finite element framework *Gridap* [4].

Example 1 (convergence against smooth solutions in 2D). Consider the unit square domain $\Omega = (0, 1)^2$ along with the following manufactured solutions

$$p(x, y) = \sin(\pi x) \cos(\pi y), \quad \text{and } \mathbf{u}(x, y) := \begin{pmatrix} \cos(\pi x) \sin(\pi y) \\ -\sin(\pi x) \cos(\pi y) \end{pmatrix}.$$

We set the left and bottom sides of the square as Γ_u and the top and right sides as Γ_p . The forcing vector \mathbf{f} and the fluid source g , as well as the (non-homogeneous) essential boundary condition on the flux, are computed based on the manufactured solutions above. We take, for this first set of examples, simply dimensional unity parameters $\kappa = \mathbf{F} = 1$ and index $r = 3.5$. The error history associated with the proposed mixed finite element method on a sequence of successively refined partitions of the domain, are presented in Table 6.1, where we also tabulate rates of error decay

DoF	h	$\ \mathbf{u} - \mathbf{u}_h\ _{3,\text{div},\Omega}$	rate	$\ p - p_h\ _{0,\Omega}$	rate	$\ P_h(\text{div } \mathbf{u}_h - g)\ _{\ell^\infty}$	it
Errors and convergence rates for $k = 0$							
45	0.7071	3.70e-01	*	8.92e-01	*	1.06e-15	3
125	0.3536	2.36e-01	0.650	3.62e-01	1.300	1.26e-15	3
405	0.1768	1.34e-01	0.810	1.25e-01	1.534	3.99e-15	3
1445	0.0884	7.18e-02	0.904	4.41e-02	1.505	7.61e-15	3
5445	0.0442	3.71e-02	0.953	1.80e-02	1.295	1.48e-14	3
21125	0.0221	1.88e-02	0.977	8.34e-03	1.106	4.33e-14	3
83205	0.0110	9.50e-03	0.989	4.10e-03	1.026	2.01e-13	3
Errors and convergence rates for $k = 1$							
144	0.7071	8.18e-02	*	2.34e-01	*	1.49e-14	3
400	0.3536	3.11e-02	1.395	5.90e-02	1.991	1.26e-14	3
1296	0.1768	9.89e-03	1.654	1.13e-02	2.387	3.69e-14	4
4624	0.0884	2.81e-03	1.818	1.95e-03	2.530	6.67e-14	4
17424	0.0442	7.48e-04	1.908	3.68e-04	2.409	1.67e-13	4
67600	0.0221	1.93e-04	1.954	8.09e-05	2.184	3.84e-13	4
266256	0.0110	4.90e-05	1.977	1.95e-05	2.052	8.43e-13	4

TABLE 6.1

Example 1. Error history against smooth manufactured solutions (errors on a sequence of successively refined grids, convergence rates, and norm of the divergence of the discrete velocity) for different polynomial degrees, and iteration count for the nonlinear Newton–Raphson solver. Here we are just using unity parameters (and $r = 3.5$) and the $\mathbf{H}^3(\text{div}, \Omega)$ and $L^2(\Omega)$ norms for velocity and pressure, respectively.

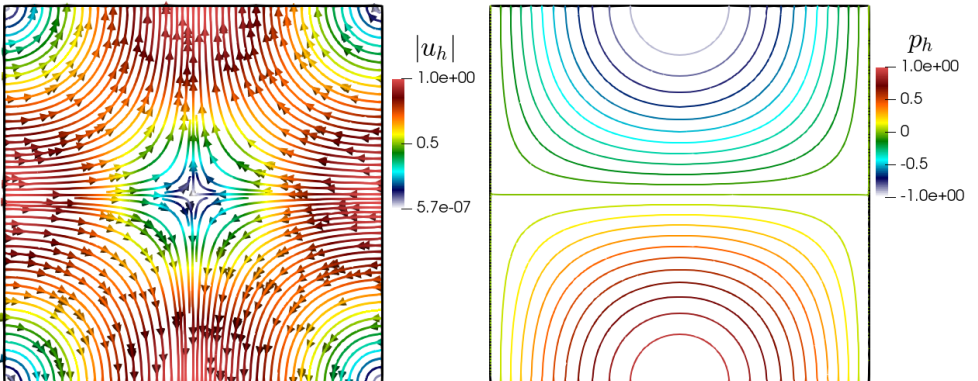


FIG. 6.1. *Example 1.* Streamlines of the approximate velocity (left) and pressure distribution (right) for the accuracy test of the Darcy–Forchheimer equations with unit parameters.

computed as $\text{rate} = \log(e_{(\bullet)}/\tilde{e}_{(\bullet)})[\log(h/\tilde{h})]^{-1}$, where e, \tilde{e} denote errors generated on two consecutive meshes of sizes h and \tilde{h} , respectively. The results indicate optimal convergence in all fields and for the two tested polynomial degrees. Moreover, a maximum of four iterations are needed by the Newton–Raphson method to reach a tolerance (either absolute or relative) of 10^{-8} on the residual. Sample approximate solutions for velocity and pressure obtained with the second-order method (with $k = 1$) are plotted in Figure 6.1. For these results, we consider the norms $\mathbf{H}^3(\text{div}, \Omega)$ and $L^2(\Omega)$ for velocity and pressure (with no parameter weighting).

Example 2 (experimental self-convergence with extreme parameters). For a second run of simulations we use the domain $\Omega = (0, 2) \times (0, 1)$ without a known analytical solution, setting the problem data as $\mathbf{f} = \mathbf{0}$, $g = 0$, mixed boundary conditions as follows $\mathbf{u} \cdot \mathbf{n} = 2.5y(1-y)$ on the left segment, $\mathbf{u} \cdot \mathbf{n} = 0$ on the top and bottom segments, and $p = 0$ on the right edge. The permeability is heterogeneous

DoF	h	$\ \mathbf{u} - \mathbf{u}_h\ _{3,\text{div},\Omega}$	rate	$\ p - p_h\ _{0,\Omega}$	rate	$\ P_h(\text{div } \mathbf{u}_h - g)\ _{\ell^\infty}$
Errors and convergence rates for $k = 0$						
36	0.7071	5.18e-01	*	1.01e+09	*	2.22e-16
84	0.3536	4.25e-01	0.285	3.88e+08	1.385	1.33e-15
240	0.1768	4.56e-01	-0.101	1.78e+08	1.127	1.35e-15
792	0.0884	2.77e-01	0.718	6.29e+07	1.499	4.00e-15
2856	0.0442	1.53e-01	0.857	1.93e+07	1.707	9.32e-15
10824	0.0221	8.29e-02	0.884	6.53e+06	1.561	2.20e-14
Errors and convergence rates for $k = 1$						
120	0.7071	4.07e-01	*	1.18e+08	*	3.02e-15
276	0.3536	3.70e-01	0.138	6.18e+07	0.929	8.07e-15
780	0.1768	2.47e-01	0.582	2.29e+07	1.434	1.39e-14
2556	0.0884	1.13e-01	1.136	7.71e+06	1.568	5.32e-14
9180	0.0442	3.74e-02	1.589	2.34e+06	1.724	2.06e-13
34716	0.0221	1.67e-02	1.159	6.33e+05	1.883	4.90e-13
DoF	h	$\ \mathbf{u} - \mathbf{u}_h\ _{\mathbf{V}}$	rate	$\ p - p_h\ _{\widehat{\mathbf{Q}}(\mathcal{T}_h)}$	rate	$\ P_h(\text{div } \mathbf{u}_h - g)\ _{\ell^\infty}$
Errors and convergence rates for $k = 0$						
36	0.7071	1.44e+03	*	7.16e+02	*	2.22e-16
84	0.3536	5.95e+02	1.276	2.67e+02	1.424	6.66e-16
240	0.1768	3.65e+02	0.705	1.14e+02	1.221	1.18e-15
792	0.0884	1.64e+02	1.153	4.08e+01	1.490	3.00e-15
2856	0.0442	5.26e+01	1.642	2.16e+01	1.352	7.55e-15
10824	0.0221	2.18e+01	1.272	1.04e+00	1.203	1.47e-14
Errors and convergence rates for $k = 1$						
120	0.7071	4.64e+02	*	1.66e+02	*	3.06e-15
276	0.3536	2.25e+02	1.044	3.62e+01	2.194	4.72e-15
780	0.1768	1.11e+02	1.017	1.29e+01	1.484	1.28e-14
2556	0.0884	3.41e+01	1.706	5.59e+00	1.211	4.45e-14
9180	0.0442	7.01e+00	2.282	2.56e+00	1.129	6.74e-14
34716	0.0221	1.16e+00	2.601	6.80e-01	1.912	1.34e-13

TABLE 6.2

Example 2. Error history against a fine-mesh reference solution (experimental errors on a sequence of successively refined grids, convergence rates, and norm of the divergence of the discrete velocity) for different polynomial degrees. Here we use $\kappa = 10^{-8}$, $F = 10^4$ (and $r = 3.5$), and the non-weighted (top rows) and parameter-weighted (bottom rows) norms for velocity and pressure.

$\kappa(\mathbf{x}) = \kappa_0(1 + \exp(-\frac{1}{2}[10y - 5 - \sin(10x)]^2))$, and we consider the more extreme parameter values $\kappa_0 = 10^{-8}$, $F = 10^4$, and $r = 3.5$. In Table 6.2 we show the error decay where we compute experimental errors against a fine-mesh reference solution $\mathbf{u}_{\text{ref}}, p_{\text{ref}}$ (with two more refinement steps than the finest level). In the first part of the table we use the non-weighted norms and we see very large errors in the pressure, a sub-optimal error decay for the velocity in the second-order case. In contrast, for the second part of the table the errors are now measured in the weighted norms associated with \mathbf{V} and $\widehat{\mathbf{Q}}(\mathcal{T}_h)$ defined in (4.1) and (4.3), respectively, where we move the scaling of the now variable permeability inside the norm definition. We recall from [5] that in the space Q_h the realisation of the required discrete weighted Laplacian operator that is the Riesz map for $\kappa^{\frac{1}{2}}H_{h,\Gamma_p}^1(\Omega)$ is as follows

$$\langle -\text{div}(\kappa(\mathbf{x})\nabla p_h), q_h \rangle = \sum_{K \in \mathcal{T}_h} (\kappa(\mathbf{x})\nabla p_h, \nabla q_h)_K + \sum_{F \in \mathcal{E}_h \cup \mathcal{E}_h^{\Gamma_p}} \frac{1}{h_F} (\kappa(\mathbf{x})[[p_h]], [[q_h]]_F),$$

where \mathcal{E}_h denotes the set of internal facets, $\mathcal{E}_h^{\Gamma_p}$ denotes the set of facets lying on the sub-boundary Γ_p , and $[[\bullet]]$ represents the jump operator across a facet (and adopt the convention that it reduces to the identity if the face lies on the boundary). In turn, for

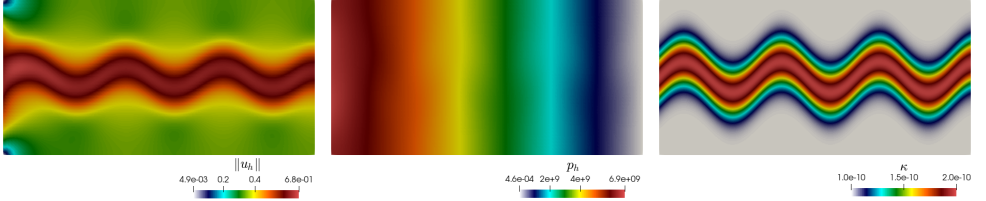


FIG. 6.2. Example 2. Sample of filtration velocity magnitude, pressure profile, and heterogeneous permeability, for the convergence test with no known analytical solution.

the space $F^{-\frac{1}{3}}W_{h,\Gamma_p}^{1,\frac{3}{2}}(\Omega)$ the natural operator (duality map) is the nonlinear discrete s -Laplacian

$$\begin{aligned} \langle -\operatorname{div}(F^{-1}|\nabla p_h|^{s-2}\nabla p_h), q_h \rangle &= \sum_{K \in \mathcal{T}_h} F^{-1}(|\nabla p_h|^{s-2}\nabla p_h, \nabla q_h)_K \\ &\quad + \sum_{F \in \mathcal{E}_h \cup \mathcal{E}_h^{\Gamma_p}} F^{-1}h_F^{1-s}(|\llbracket p_h \rrbracket|^{s-2}\llbracket p_h \rrbracket, \llbracket q_h \rrbracket)_F, \end{aligned}$$

with $s = \frac{3}{2}$ (see, e.g., [9]). However, since we require a linear operator to define the preconditioner-induced norm, we use instead the following linearisation around the reference pressure

$$\begin{aligned} \sum_{K \in \mathcal{T}_h} F^{-1}(|\nabla p_{\text{ref}}|^{s-2}\nabla p_h, \nabla q_h)_K &+ \sum_{F \in \mathcal{E}_h \cup \mathcal{E}_h^{\Gamma_p}} F^{-1}(s-1)h_F^{1-s}(|\llbracket p_{\text{ref}} \rrbracket|^{s-2}\llbracket p_h \rrbracket, \llbracket q_h \rrbracket)_F \\ &+ \sum_{K \in \mathcal{T}_h} F^{-1}(s-2)(|\nabla p_{\text{ref}}|^{s-4}(\nabla p_{\text{ref}} \cdot \nabla p_h), (\nabla p_{\text{ref}} \cdot \nabla q_h))_K. \end{aligned}$$

It is observed that the rates remain optimal, as anticipated by Theorem 4.6. Snapshots of the numerical solutions for the lowest-order scheme are shown in Figure 6.2.

Example 3 (application to filtration in highly permeable media). In this test example, we simulate typical flow through a porous domain with large obstacles. The domain has length of 0.1 m and includes seven circular cylinders of different sizes. The permeability is not isotropic, but a tensor (that also needs to be scaled with fluid viscosity). In its principal direction frame, we have

$$\kappa_0 = \frac{1}{\nu} \begin{pmatrix} \kappa_1 & 0 \\ 0 & \kappa_2 \end{pmatrix}, \quad (6.1)$$

with $\nu = 10^{-6} \text{ m}^2\text{s}^{-1}$, $\kappa_1 = 5 \cdot 10^{-10} \text{ m}^2$ and $\kappa_2 = 10^{-10} \text{ m}^2$, and the tensor is rotated by $4.7^\circ = 0.082 \text{ rad}$ from the x -axis giving,

$$\kappa = \mathbf{R}\kappa_0\mathbf{R}^t, \quad \text{where} \quad \mathbf{R} = \begin{pmatrix} \cos(\theta) & -\sin(\theta) \\ \sin(\theta) & \cos(\theta) \end{pmatrix}.$$

The external force \mathbf{f} has magnitude $1.3 \cdot 10^{-5} \text{ ms}^{-2}$ and it points in the x direction, and we assume zero fluid source $g = 0$. We consider an inlet boundary on the bottom left circular arc, on which we impose a radial inlet velocity $\mathbf{u} \cdot \mathbf{n} = \frac{1}{4}\mathbf{x}/|\mathbf{x}| \text{ m/s}$; an outlet boundary on the upper right circular arc, on which we impose $p = 0$, and on the remainder of the boundary (including the obstacles) we set $\mathbf{u} \cdot \mathbf{n} = 0$. Parameter values

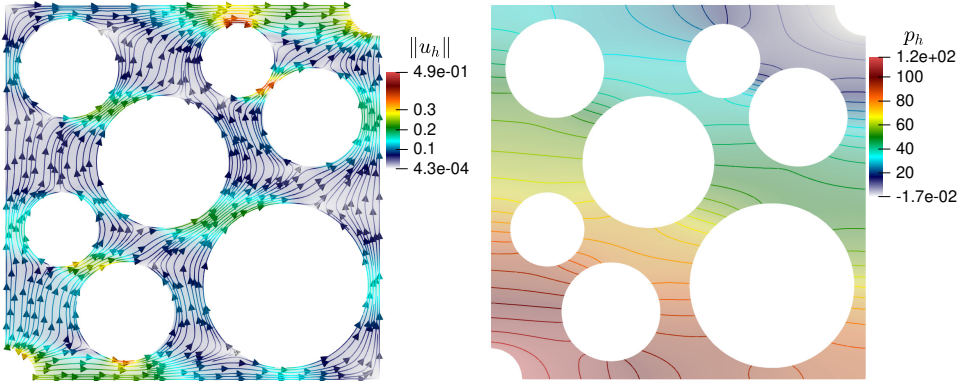


FIG. 6.3. Example 3. Streamlines of the approximate velocity coloured by velocity magnitude (left) and contours of pressure distribution (right), for the flow across obstacles using the Darcy–Forchheimer equations with anisotropic permeability. A second-order scheme ($k = 1$) is used.

and flow configurations have been adapted from [20]. The unstructured triangular mesh has 26,184 elements and we use for this test a second-order scheme (setting $k = 1$), giving a total number of 197,296 DoFs. The remaining parameters are the Forchheimer coefficient and index, taken here as $F = 1 \text{ m}^{-1} \cdot \rho$ with $\rho = 10^3 \text{ kg m}^{-3}$, and $r = 3$. Finally, we note that the use of a Forchheimer correction term is justified in this case since the Forchheimer threshold coefficient (recall that the permeability coefficient is already scaled with viscosity in (6.1))

$$F_0 = \kappa_{\max} F |\mathbf{u}|$$

is 0.245 (the rule suggested in [35], see also [15], specifies that it has to be larger than 0.1) when taking for $|\mathbf{u}|$ its maximum value over Ω (not known a priori but computed to be 0.49). We depict in Figure 6.3 the approximate solutions, indicating the expected filtration patterns in porous media with large obstacles. The Newton–Raphson solver took eight iterations to converge.

Example 4 (operator preconditioning for the linearised problem). To conclude we conduct a series of computations where the permeability κ and the Forchheimer coefficient r are varied over several orders of magnitude, and the Forchheimer index F is also varied. This is done again using the domain $\Omega = (0, 1)^2$, the lowest-order finite element family, and mixed boundary conditions as in Example 1. The performance of the numerical method is assessed by comparing an estimate of the condition number of the linearised system matrix (5.3) preconditioned with the weighted duality map (5.4). Table 6.3 illustrates the robustness of the proposed preconditioner across the parametric space. Additionally, the performance of the preconditioner corresponding to the weighted Riesz map (5.8) has also been illustrated in Table 6.4, which seems to perform slightly better than (5.4). However, we remark that, quite similarly to [5], the map (5.4) will be preferable in a multiphysics context where the scaling of the divergence component of the velocity block is not convenient. Another crucial point worth mentioning is that, although extreme parametric values of both κ and F are considered, and they have the opposite limiting directions, with more refinement of the mesh, effect of κ seems to dominate the effects of F in the sense of higher condition numbers.

r	κ	F	h			r	κ	F	h			r	κ	F	h					
			2^{-2}	2^{-3}	2^{-4}				2^{-2}	2^{-3}	2^{-4}				2^{-2}	2^{-3}	2^{-4}			
3	10^{-8}	1	6.61	7.52	8.01	10^{-8}	1	6.61	7.52	8.01	10^{-8}	1	6.61	7.52	8.01	10^{-8}	1	6.61	7.52	8.01
		10^3	6.61	7.52	8.01		10^3	6.61	7.52	8.01		10^3	6.61	7.52	8.01		10^3	6.61	7.52	8.01
		10^9	6.59	7.50	8.00		10^9	6.61	7.52	8.01		10^9	6.61	7.52	8.01		10^9	6.61	7.52	8.01
	10^{-4}	1	6.41	6.77	6.78	10^{-4}	1	6.41	6.77	6.78	10^{-4}	1	6.41	6.77	6.78	10^{-4}	1	6.41	6.77	6.78
		10^3	6.41	6.77	6.78		10^3	6.41	6.77	6.78		10^3	6.41	6.77	6.78		10^3	6.41	6.77	6.78
		10^9	4.27	4.74	4.86		10^9	6.41	6.77	6.78		10^9	6.41	6.77	6.78		10^9	6.41	6.77	6.78
	1	1	2.08	2.11	2.13	4	1	2.08	2.11	2.13	5	1	2.08	2.11	2.13	1	1	2.08	2.11	2.13
		10^3	1.79	1.93	2.03		1	10^3	2.08	2.11	2.13	10^3	2.08	2.11	2.13	10^3	2.08	2.11	2.13	
		10^9	4.25	4.69	4.78		1	10^9	2.08	2.11	2.13	10^9	2.08	2.11	2.13	10^9	2.08	2.11	2.13	

TABLE 6.3

Example 4. Estimated condition number of the preconditioned system matrix of the linearised Darcy–Forchheimer equations using the preconditioner induced by (5.4).

r	κ	F	h			r	κ	F	h			r	κ	F	h					
			2^{-2}	2^{-3}	2^{-4}				2^{-2}	2^{-3}	2^{-4}				2^{-2}	2^{-3}	2^{-4}			
3	10^{-8}	1	2.63	2.63	2.63	10^{-8}	1	2.63	2.63	2.63	10^{-8}	1	2.63	2.63	2.63	10^{-8}	1	2.63	2.63	2.63
		10^3	2.63	2.63	2.63		10^3	2.63	2.63	2.63		10^3	2.63	2.63	2.63		10^3	2.63	2.63	2.63
		10^9	2.62	2.63	2.63		10^9	2.63	2.63	2.63		10^9	2.63	2.63	2.63		10^9	2.63	2.63	2.63
3	10^{-4}	1	2.63	2.63	2.63	4	1	2.63	2.63	2.63	5	1	2.63	2.63	2.63	5	1	2.63	2.63	2.63
		10^3	2.63	2.63	2.63		10^3	2.63	2.63	2.63		10^3	2.63	2.63	2.63		10^3	2.63	2.63	2.63
		10^9	1.34	1.34	1.36		10^9	2.63	2.63	2.63		10^9	2.63	2.63	2.63		10^9	2.63	2.63	2.63
[4]	1	2.63	2.63	2.63	1	1	2.63	2.63	2.63	1	1	2.63	2.63	2.63	1	1	2.63	2.63	2.63	
	10^3	2.18	2.32	2.42		10^3	2.63	2.63	2.63		10^3	2.63	2.63	2.63		10^3	2.63	2.63	2.63	
	10^9	1.31	1.29	1.27		10^9	2.63	2.63	2.63		10^9	2.63	2.63	2.63		10^9	2.63	2.63	2.63	

TABLE 6.4

Example 4. Estimated condition number of the preconditioned system matrix of the linearised Darcy–Forchheimer equations using the preconditioner induced by (5.8).

REFERENCES

- [1] R. AL DBAISY AND T. SAYAH, *Iterative scheme for the Darcy–Forchheimer problem with pressure boundary condition*, WSEAS Transactions on Heat and Mass Transfer, 19 (2024), pp. 94–106.
- [2] D. N. ARNOLD, R. S. FALK, AND R. WINTHER, *Preconditioning in $H(\text{div})$ and applications*, Mathematics of Computation, 66 (1997), pp. 957–984.
- [3] J. D. AUDU, F. FAIRAG, AND K. MUSTAPHA, *Mixed finite element analysis for generalized Darcy–Forchheimer model in porous media*, Journal of Computational and Applied Mathematics, 353 (2019), pp. 191–203.
- [4] S. BADIA, A. F. MARTÍN, AND F. VERDUGO, *GridapDistributed: a massively parallel finite element toolbox in Julia*, Journal of Open Source Software, 7 (2022), p. 4157.
- [5] T. BÆRLAND, M. KUCHTA, K.-A. MARDAL, AND T. THOMPSON, *An observation on the uniform preconditioners for the mixed Darcy problem*, Numerical Methods for Partial Differential Equations, 36 (2020), pp. 1718–1734.
- [6] J. W. BARRETT AND W. B. LIU, *Finite element approximation of the p -laplacian*, Mathematics of computation, 61 (1993), pp. 523–537.
- [7] D. BOFFI, F. BREZZI, AND M. FORTIN, *Mixed finite element methods and applications*, vol. 44, Springer, 2013.
- [8] W. M. BOON, M. KUCHTA, K.-A. MARDAL, AND R. RUIZ-BAIER, *Robust preconditioners for perturbed saddle-point problems and conservative discretizations of Biot’s equations utilizing total pressure*, SIAM Journal on Scientific Computing, 43 (2021), pp. B961–B983.
- [9] E. BURMAN AND A. ERN, *Discontinuous galerkin approximation with discrete variational principle for the nonlinear Laplacian*, Comptes Rendus. Mathématique, 346 (2008), pp. 1013–1016.
- [10] R. CARABALLO, C. W. IN, A. F. MARTÍN, AND R. RUIZ-BAIER, *Robust finite element methods and solvers for the Biot–Brinkman equations in vorticity form*, Numerical Methods for Partial Differential Equations, 40 (2024), pp. e23083(1–26).
- [11] S. CAUCAO AND M. DISCACCIA, *A mixed FEM for the coupled Brinkman–Forchheimer/Darcy problem*, Applied Numerical Mathematics, 190 (2023), pp. 138–154.
- [12] S. CAUCAO, M. DISCACCIA, G. N. GATICA, AND R. OYARZÚA, *A conforming mixed finite ele-*

ment method for the Navier–Stokes/Darcy–Forchheimer coupled problem, ESAIM: Mathematical Modelling and Numerical Analysis, 54 (2020), pp. 1689–1723.

- [13] A. ERN AND J.-L. GUERMOND, *Finite elements I: Approximation and interpolation*, vol. 72, Springer Nature, 2021.
- [14] I. FARAGÓ AND J. KARÁTSON, *Numerical solution of nonlinear elliptic problems via preconditioning operators: Theory and applications*, vol. 11, Nova Publishers, 2002.
- [15] A. FUMAGALLI AND F. S. PATACCINI, *Model adaptation for non-linear elliptic equations in mixed form: existence of solutions and numerical strategies*, ESAIM: Mathematical Modelling and Numerical Analysis, 56 (2022), pp. 565–592.
- [16] G. N. GATICA, *A simple introduction to the mixed finite element method*, Theory and Applications. Springer Briefs in Mathematics. Springer, London, (2014).
- [17] G. N. GATICA, S. MEDDAHI, AND R. RUIZ-BAIER, *An L^p spaces-based formulation yielding a new fully mixed finite element method for the coupled Darcy and heat equations*, IMA Journal of Numerical Analysis, 42 (2022), pp. 3154–3206.
- [18] V. GIRAUT AND M. F. WHEELER, *Numerical discretization of a Darcy–Forchheimer model*, Numerische Mathematik, 110 (2008), pp. 161–198.
- [19] A. GRILLO, M. CARFAGNAY, AND S. FEDERICOZ, *The Darcy–Forchheimer law for modelling fluid flow in biological tissues*, Theoretical and Applied Mechanics, 41 (2014), pp. 283–322.
- [20] P. HASSARD, I. TURNER, AND D. LESTER, *Comparison of lattice Boltzmann and boundary element methods for Stokes and visco-inertial flow in a two-dimensional porous medium*, Transport in Porous Media, 150 (2023), pp. 675–707.
- [21] F. S. HIRA, Q. RUBBAB, I. AHMAD, AND A. H. MAJEE, *Advanced computational modeling of Darcy–Forchheimer effects and nanoparticle-enhanced blood flow in stenosed arteries*, Engineering Applications of Artificial Intelligence, 152 (2025), p. 110737.
- [22] Q. HONG AND J. KRAUS, *Parameter-robust stability of classical three-field formulation of biot's consolidation model*, Electronic Transactions on Numerical Analysis, 48 (2018), pp. 202–226.
- [23] Q. HONG, J. KRAUS, M. LYMBERY, AND F. PHILO, *Conservative discretizations and parameter-robust preconditioners for Biot and multiple-network flux-based poroelasticity models*, Numerical Linear Algebra with Applications, 26 (2019), p. e2242.
- [24] J. HUANG, L. CHEN, AND H. RUI, *Multigrid methods for a mixed finite element method of the Darcy–Forchheimer model*, Journal of Scientific Computing, 74 (2018), pp. 396–411.
- [25] A. KLAWONN, *An optimal preconditioner for a class of saddle point problems with a penalty term. Part II: General theory*, Tech. Rep. 14/95, Westfälische Wilhelms-Universität Münster, Germany, 1995.
- [26] S. LIU, A. AHMADI-SENICHAULT, A. BEN-ABDELAHED, H. YAO, AND J. LACHAUD, *Experimental investigation and DEM-CFD analysis of Darcy–Forchheimer flows in randomly packed bed systems of wood particles*, International Journal of Heat and Mass Transfer, 235 (2024), p. 126229.
- [27] H. LÓPEZ, B. MOLINA, AND J. J. SALAS, *Comparison between different numerical discretizations for a Darcy–Forchheimer model*, Electronic Transactions on Numerical Analysis, 34 (2009), pp. 187–203.
- [28] K.-A. MARDAL AND R. WINTHORP, *Preconditioning discretizations of systems of partial differential equations*, Numerical Linear Algebra with Applications, 18 (2011), pp. 1–40.
- [29] S. A. MATHIAS, J. N. McELWAINE, AND J. G. GLUYAS, *Heat transport and pressure buildup during carbon dioxide injection into depleted gas reservoirs*, Journal of Fluid Mechanics, 756 (2014), pp. 89–109.
- [30] V. MAZ'YA AND J. ROSSMANN, *Elliptic Equations in Polyhedral Domains*, no. 162, American Mathematical Soc., 2010.
- [31] H. PAN AND H. RUI, *Mixed element method for two-dimensional Darcy–Forchheimer model*, Journal of Scientific Computing, 52 (2012), pp. 563–587.
- [32] E. PIERSANTI, J. J. LEE, T. THOMPSON, K.-A. MARDAL, AND M. E. ROGNES, *Parameter robust preconditioning by congruence for multiple-network poroelasticity*, SIAM Journal on Scientific Computing, 43 (2021), pp. B984–B1007.
- [33] J. SCHÖBERL AND W. ZULEHNER, *Symmetric indefinite preconditioners for saddle point problems with applications to PDE-constrained optimization problems*, SIAM Journal on Matrix Analysis and Applications, 29 (2007), pp. 752–773.
- [34] P. S. VASSILEVSKI AND U. VILLA, *A block-diagonal algebraic multigrid preconditioner for the Brinkman problem*, SIAM Journal on Scientific Computing, 35 (2013), pp. S3–S17.
- [35] Z. ZENG AND R. GRIGG, *A criterion for non-Darcy flow in porous media*, Transport in Porous Media, 63 (2006), pp. 57–69.